Research Square

Preprints are preliminary reports that have not undergone peer review.
They should not be considered conclusive, used to inform clinical practice,
or referenced by the media as validated information.

Genomic dissection of Bwr-12 identifies an ancestral receptor-like protein underlying resistance to multiple bacterial wilt strains in tomato

Seon-In Yeom

sunin78@gnu.ac.kr

Gyeongsang National University

Ji-Su Kwon

Department of Horticulture, Division of Applied Life Science (BK21 Four Program), Institute of Agriculture & Life Science, Gyeongsang National University https://orcid.org/0000-0002-9864-0318

Junesung Lee

Department of Horticulture, Division of Applied Life Science (BK21 Four Program), Institute of Agriculture & Life Science, Gyeongsang National University https://orcid.org/0000-0002-8076-7935

Myung-Shin Kim

Myungji University https://orcid.org/0000-0002-5967-4347

Boseul Park

Department of Horticulture, Division of Applied Life Science (BK21 Four Program), Institute of Agriculture & Life Science, Gyeongsang National University

Seungyong Lee

Department of Horticulture, Division of Applied Life Science (BK21 Four Program), Institute of Agriculture & Life Science, Gyeongsang National University

Seoyeon Im

Department of Horticulture, Division of Applied Life Science (BK21 Four Program), Institute of Agriculture & Life Science, Gyeongsang National University

Janguk Huh

Department of Biosciences and Bioinformatics, Myongji University https://orcid.org/0009-0003-7007-3715

Junseok Lee

Department of Biosciences and Bioinformatics, Myongji University https://orcid.org/0009-0008-7493-5905

Jin Ho Yang

Korea Research Institute of Bioscience and Biotechnology

Jin-hee Jeong

Nulla Bio R&D Center, Nulla Bio Inc https://orcid.org/0000-0001-6088-378X

Hye-Young Lee

Gyeongsang National University

Je Min Lee

Kyungpook National University https://orcid.org/0000-0002-0446-1336

Chang-Sik Oh

Department of Agricultural Biotechnology, College of Agriculture and Life Science, Seoul National University https://orcid.org/0000-0002-2123-862X

Hyun-Soon Kim

Korea Research Institute of Bioscience and Biotechnology

Yong-Min Kim

Korea Research Institute of Bioscience and Biotechnology https://orcid.org/0000-0001-9210-5843

Seon-Woo Lee

Dong-A University https://orcid.org/0000-0001-6142-7612

Won-Hee Kang

Department of Horticulture, Division of Applied Life Science (BK21 Four Program), Institute of Agriculture & Life Science, Gyeongsang National University

---

Article

Keywords:

Posted Date: November 19th, 2026

DOI: https://doi.org/10.21203/rs.3.rs-11765631/v1

License: This work is licensed under a Creative Commons Attribution 4.0 International License. Read Full License

Additional Declarations: There is **NO** Competing Interest.

Genomic dissection of *Bwr-12* identifies an ancestral receptor-like protein underlying resistance to multiple bacterial wilt strains in tomato

Authors

Ji-Su Kwon[1*], Junesung Lee[1*], Myung-Shin Kim[2*], Boseul Park[1], Seungyong Lee[1], Seoyeon Im[1], Janguk Huh[2], Junseok Lee[2], Jin Ho Yang[3], Jin-hee Jeong[4], Hye-Young Lee[1], Je Min Lee[5], Chang-Sik Oh[6], Hyun-Soon Kim[3], Yong-Min Kim[7], Seon-Woo Lee[8], Won-Hee Kang[1†] & Seon-In Yeom[1†]

Affiliations

[1] Department of Horticulture, Division of Applied Life Science (BK21 Four Program), Institute of Agriculture & Life Science, Gyeongsang National University, Jinju 52828, Republic of Korea

[2] Department of Biosciences and Bioinformatics, Myongji University, Yongin 17058, Republic of Korea

[3] Plant Systems Engineering Research Center, Korea Research Institute of Bioscience and Biotechnology, 125 Gwahak-ro, Daejeon 34141, Korea

[4] Nulla Bio R&D Center, Nulla Bio Inc, Jinju 52828, Republic of Korea

[5] Department of Horticultural Science, Kyungpook National University, Daegu 41566, Republic of Korea

[6] Department of Agricultural Biotechnology, College of Agriculture and Life Sciences, Seoul National University, Seoul 08826, Republic of Korea

[7] Plant Systems Engineering Research Center, Korea Research Institute of Bioscience and Biotechnology (KRIBB), Daejeon 34141, Republic of Korea

[8] Department of Applied Bioscience and Institute of Agricultural Life Sciences, Dong-A University, Busan 49315, Republic of Korea

*These authors contributed equally: Ji-Su Kwon, Junesung Lee, Myung-Shin Kim

†Corresponding author. E-mail: sunin78@gnu.ac.kr, whkang@gnu.ac.kr

Abstract

Bacterial wilt, caused by the *Ralstonia solanacearum* species complex, affects over 450 plant species worldwide and is increasingly severe under climate change. Despite decades of breeding efforts, the molecular basis of durable and broad-spectrum resistance has remained unresolved. Here, we assembled a chromosome-scale genome of the resistant tomato breeding line ‘Hawaii7996’ and integrated resequencing, comparative genomics, and transcriptome profiling with functional validation. This multi-omics framework resolved the long-standing *Bwr-12* locus and identified *SlBWR12*, a receptor-like protein that makes a major contribution to bacterial wilt resistance. CRISPR–Cas9-mediated knockout of *SlBWR12* substantially reduced resistance, whereas overexpression conferred strong resistance in susceptible tomato backgrounds. Importantly, heterologous expression of *SlBWR12* conferred resistance in *Nicotiana benthamiana* and potato, indicating conserved functionality beyond species boundaries. Evolutionary analyses revealed that *SlBWR12* is retained in wild tomato relatives but frequently pseudogenized in cultivated varieties, reflecting erosion of resistance during domestication. Together, these findings establish *SlBWR12* as a transferable gene-level resource for restoring bacterial wilt resistance and support its use in gene-based breeding and genome editing across crops.

Introduction

Bacterial wilt, caused by the *Ralstonia solanacearum* species complex (RSSC), is one of the most pervasive and climate-sensitive bacterial diseases threatening agricultural sustainability worldwide[1,2]. This soil-borne pathogen infects more than 450 host species, including economically important solanaceous crops such as tomato, potato, and pepper, and causes global yield losses exceeding US$1 billion annually[3,4]. Its incidence is rapidly intensifying under global warming, as the pathogen expands into temperate regions, evolves tolerance to cooler temperatures, and diversifies into new virulent strains[5]. Particularly in East and Southeast Asia, high temperature and humidity favor pathogen persistence, leading to increasingly frequent and severe outbreaks[6].

The management of bacterial wilt remains one of the most intractable challenges in crop production[7]. The pathogen's persistence in soil and water, extensive host range, and latent infection cycle make chemical and cultural control strategies largely ineffective[8,9]. Even commercial cultivars bred for resistance often fail under field conditions due to the pathogen's genetic heterogeneity and the environment-dependent expression of resistance[10]. Consequently, despite decades of breeding efforts, the development of cultivars with durable and broad-spectrum resistance has remained a major challenge[11].

At the molecular level, only a limited number of genetic determinants of bacterial wilt resistance have been identified and functionally characterized across plant species. These include the TIR-NLR pair *RRS1–RPS4*[12]. and the receptor-like kinase *ERECTA*[13]. in *Arabidopsis thaliana*, the TIR-NLR receptor *Roq1* from *Nicotiana benthamiana*, which recognizes the *Ralstonia* effector RipB[14], and more recently, the leucine-rich repeat receptor-like kinase *AhBWR15* in peanut[15]. In tomato, however, despite extensive genetic mapping of bacterial wilt resistance, the endogenous causal genes underlying major resistance loci have remained elusive. Accordingly, breeding has continued to rely largely on resistant donor

germplasm and quantitative trait loci (QTLs), whose effects are often strongly influenced by pathogen strain and environmental conditions[16].

In tomato, genetic resistance to bacterial wilt has been investigated since the 1960s, with *Solanum lycopersicum* 'Hawaii7996' serving as the major source of resistance in breeding programs. Although it is presumed to have originated from wild relatives, its precise pedigree remains uncertain[17,18]. Since then, resistance to RSSC has been repeatedly mapped to two quantitative trait loci (QTLs): *Bwr-6* which confers partial and strain-specific resistance with relatively minor effects, and *Bwr-12* , which has been associated with major and relatively stable resistance effects across multiple environments and *Ralstonia* strains[19].

Despite extensive mapping, the causal genes underlying these loci remain unidentified, leaving breeding programs reliant on indirect QTL-based selection without a defined molecular basis for resistance[20,21]. This knowledge gap reflects both technical and biological constraints, including the reliance on susceptible reference genomes, the narrow genetic diversity captured by biparental mapping, and the extensive genetic heterogeneity within RSSC. Pinpointing the causal gene(s) underlying major resistance QTLs would enable a shift from empirical QTL selection to predictive, gene-based improvement with immediate translational utility.

Here, leveraging the newly assembled 'HW7996' genome, we identified *SlBWR12,* a receptor-like protein (RLP) encoded within the *Bwr-12* locus, as a major-effect gene contributing to bacterial wilt resistance in tomato. We further determined that the functional *SlBWR12* allele represents an ancestral resistance-associated allele retained in wild relatives but frequently disrupted in cultivated tomato, underscoring the importance of conserving wild genetic diversity for future breeding. By filling this critical knowledge gap, we identify and functionally validate *SlBWR12* as, to our knowledge, the first endogenous tomato gene cloned from a naturally occurring bacterial wilt resistance QTL and genetically validated by reciprocal

loss- and gain-of-function analyses.

Results

High-quality genome assembly and structural features of ‘Hawaii7996’

To identify the genetic basis of bacterial wilt resistance, we generated a chromosome-scale reference genome for the resistant breeding line Hawaii7996 (‘HW7996’). Using 62.96 Gb (76.78×) of Oxford Nanopore long reads, 43.95 Gb (53.6×) of Illumina short reads, and 30.27 Gb (36.91×) of Hi-C data (Supplementary Table 1), we assembled an 819.6 Mb genome with a contig N50 of 14.5 Mb and a scaffold N50 of 66.6 Mb (L50 = 6), representing 93.5% of the estimated genome size of ~876.5 Mb (Table 1, Supplementary Table 2; Supplementary Fig. 1). The assembly was anchored into 13 pseudomolecules (12 chromosomes plus chr00) using the *S. lycopersicum* ‘Heinz1706’ (SL4.0) reference genome (Supplementary Fig. 1c).

Repetitive elements accounted for 73.58% of the genome, dominated by long terminal repeat retrotransposons (LTR-RTs) of the Gypsy (40.49%) and Copia (9.97%) families (Supplementary Fig. 1e). We used transcriptomic, homology-based, and *ab initio* evidence to predict 35,909 protein-coding genes with 98.3% BUSCO completeness at the assembly level and 92.5% at the gene-model level. Functional annotation of 30,223 genes (84.17%) confirmed the assembly’s high accuracy and biological completeness (Table 1).

Genome alignment of ‘HW7996’ with *S. lycopersicum* ‘Heinz1706’ and *S. pimpinellifolium* ‘LA2093’ revealed extensive macrosyntenic conservation, with only minor structural variations on chromosomes 4, 6, 11, and 12 (Supplementary Fig. 1d,f). We identified predominantly small- to medium-scale polymorphisms, with higher divergence in interspecific (‘HW7996’ vs. ‘LA2093’) vs. intraspecific (‘HW7996’ vs. ‘Heinz1706’) comparisons. Thus, the ‘HW7996’ genome provides a high-quality, chromosome-level reference and a robust framework for dissecting the molecular architecture of bacterial wilt resistance in tomato and related Solanaceae crops.

The *Bwr-12* locus contains four receptor-like candidate genes for bacterial wilt resistance

To characterize the genetic architecture of bacterial wilt resistance, we anchored previously reported QTL markers[19] onto the 'HW7996' reference genome, identifying two loci (*Bwr-6;* ~1.9 Mb on chromosome 6, and *Bwr-12;* ~2 Mb on chromosome 12) (Fig. 1a; Supplementary Table 3). Using whole-genome variant profiling of 18 tomato accessions (7 resistant and 11 susceptible), we found an average of 4.36 million variants per accession, including 3.84 million single-nucleotide polymorphisms (SNPs) (Supplementary Table 1). Variant patterns in the *Bwr-12* region of resistant accessions exhibited low sequence diversity compared to the high SNP densities in the genomes of susceptible accessions. We determined that the genomic segment of the *Bwr-12* region with the largest difference in polymorphism between resistant and susceptible accessions comprised a ~224 kb interval containing 26 genes (Fig. 1b,c; Supplementary Table 4; Supplementary Fig. 2).

To test whether this interval was supported by independent genetic evidence, we fine-mapped the locus with F_5 recombinant inbred lines (RILs) from an 'HW7996' × 'E6203' cross (Supplementary Fig. 3). The resistant recombinants '226-24' ($P = 2.04 \times 10^{-16}$ vs. 'E6203') and '346-9' (mean disease severity index, DSI = 1.6, $P = 0.00055$ vs. 'E6203') retained the 'HW7996' segment spanning the diagnostic marker RsR12-1[22], whereas the susceptible recombinants '283-28' (mean DSI = 3.9, $P = 1.4 \times 10^{-8}$ vs. 'HW7996') and '56-16' (mean DSI = 3.4, $P = 1.4 \times 10^{-8}$ vs. 'HW7996') carried the 'HW7996' segment across the downstream part of the QTL yet remained fully susceptible, excluding that region. These breakpoints delimited *Bwr-12* to a 201.8 kb interval of 28 genes (Supplementary Fig. 3; Supplementary Table 5), which overlapped the 224 kb variant-defined interval (26 genes) by 171.5 kb (Fig. 1b,c; Supplementary Fig. 2). These results suggest that whole-genome variant profiling and

146 independent genetic mapping delimit the same region.

147 To prioritize candidates within this delimited interval, we integrated sequence variation
148 profiles with transcriptome data from two independent infection assays on stem and root
149 tissues of 'HW7996' and the susceptible 'M82' at 5 days post-inoculation (dpi)[23]. Candidate
150 selection required all three criteria: sequence conservation across resistant accessions,
151 sequence divergence between resistant and susceptible accessions, and higher expression
152 in resistant than susceptible accessions upon infection, excluding all other genes in the interval
153 (Supplementary Fig. 4). Only four genes (*SlyHW12g003710, SlyHW12g003720,*
154 *SlyHW12g003730*, and *SlyHW12g003740*) met these criteria, showing consistent
155 upregulation in resistant vs. susceptible accessions (Fig. 1d; Supplementary Table 6). By
156 resequencing, we confirmed complete coding sequences for all four genes in the genomes of
157 resistant accessions but extensive polymorphisms and nonsynonymous variants in
158 susceptible accessions (Fig. 1e). All four encode RLPs, a class of cell-surface immune
159 receptors mediating pathogen perception (Supplementary Fig. 5a). *SlyHW12g003730*, with
160 the highest expression, was the top resistance gene candidate (Fig. 1f).

161 In combination, the genomic and transcriptomic analyses reduced the *Bwr-12* interval
162 of interest from ~2 Mb to a compact ~40 kb segment containing four infection-responsive RLPs,
163 defining the genes for functional validation. To assess allelic diversity in *SlyHW12g003730*,
164 we used gene-specific sequences to determine that all susceptible accessions carried indels
165 or frameshifts introducing premature stop codons in *SlyHW12g003730* (Supplementary Fig.
166 5b).

167 The chromosome 6 QTL (*Bwr-6*), previously associated with strain-dependent
168 bacterial wilt resistance, encompassed a broader and genetically more complex interval.
169 Guided by previously established QTL markers we selected only accessions with clearly
170 defined resistant or susceptible genotypes linked to *Bwr-6*, and resequencing of these 11

accessions (5 resistant and 6 susceptible) delineated four distinct candidate subregions (Extended Data Fig. 1a; Supplementary Tables 1 and 11). Resistant accessions showed local sequence conservation within these regions, whereas susceptible accessions exhibited greater sequence polymorphism (Extended Data Fig. 1b,c; Supplementary Table 7). To further characterize these candidate subregions, we examined the functional annotations and infection-responsive expression profiles of the 140 genes located within them. Fourteen genes met the differential-expression criteria used in this study (Supplementary Table 8), and the annotated genes represented diverse functional classes, including receptor- and kinase-related proteins, stress-associated proteins, and genes involved in other cellular processes (Extended Data Fig. 1d,e). However, no single gene was consistently prioritized by the combined positional, functional, and expression evidence. These results indicate that *Bwr-6* remains a genetically complex, multi-sublocus QTL region requiring further fine-mapping and functional validation. In contrast, functional analyses of the *Bwr-12* locus identified *SlBWR12* as a major-effect resistance gene.

***SlBWR12* confers resistance to multiple bacterial wilt strains**

We generated CRISPR-Cas9 knockouts of the four candidate RLP genes in the delimited *Bwr-12* locus in 'HW7996'. We obtained loss-of-function alleles for *SlyHW12g003710* (hw3710), *SlyHW12g003720* (hw3720), *SlyHW12g003730* (*SlBWR12*), and *SlyHW12g003740* (hw3740), with two independent knockout lines for *SlyHW12g003730* (*SlBWR12*-CR1 and *SlBWR12*-CR2) (Fig. 2a). Sequencing and sequence alignment of on-target PCR amplicons confirmed frameshift mutations disrupting conserved domains in all four candidate genes, with divergence points marked in Supplementary Fig. 6. Transgene-free homozygous lines were recovered in the T_2 and T_3 generations which were tested in bacterial wilt resistance assays. Genome-edited tomato lines targeting each of the four candidate RLP genes showed no

obvious developmental abnormalities, and the measured growth and fruit-related traits did not differ significantly from ‘HW7996’ under our experimental conditions (Supplementary Fig. 7a,b). Notably, disruption of *SlyHW12g003730* (*SlBWR12*) in the *SlBWR12*-CR1 line did not result in detectable changes in fruit weight, diameter, or height compared with ‘HW7996’.

The wild-type (WT) resistant ‘HW7996’ and susceptible ‘Moneymaker’ (‘MM’) plants and individual knockout lines were inoculated with *R. pseudosolanacearum* (Ral) strain SL1944 (phylotype I; tobacco isolate) by soil drenching. Only plants with knockouts of *SlyHW12g003730* (*SlBWR12*-CR1 or *SlBWR12*-CR2) showed complete wilting, phenotypically indistinguishable from the susceptible control ‘MM’, whereas ‘HW7996’ was resistant (Fig. 2b). Disease progression was evaluated over 20 days using DSI (0–4 scale). *SlBWR12* mutants showed significantly higher wilt scores than ‘HW7996’ (repeated-measures ANOVA, $P < 0.01$; Tukey’s honestly significant difference (HSD) at 18 dpi, $P < 0.05$; Fig. 2c). Bacterial population assays corroborated these observations. At 3 and 4 dpi, bacterial titers in *SlBWR12* mutants were 3.9–7.0 × 10^8 colony-forming units (CFU) cm^{-2}, levels indistinguishable from ‘MM’ but ~100-fold higher than ‘HW7996’ (Student’s t-test, $P < 0.001$; Fig. 2d). Therefore, the *SlyHW12g003730* gene, now designated *SlBWR12* (*Solanum lycopersicum BWR-12*), was identified as a major-effect resistance gene within the *Bwr-12* QTL.

To test whether *SlBWR12* contributes to resistance against multiple RSSC strains, infection of *SlBWR12* knockout lines with Ral SL882 (phylotype I; eggplant isolate) and Ral GMI1000 (phylotype I; tomato isolate) isolates led to complete wilting comparable to ‘MM’, indicating a substantial loss of resistance to both strains. In contrast, ‘HW7996’ and knockouts of the other three RLP candidates were strongly resistant to all three strains (Fig. 2e). Thus, loss of *SlBWR12* substantially compromised resistance to the tested strains, supporting *SlBWR12* as a major-effect resistance component encoded within the *Bwr-12* locus.

Consistent with these functional data, the *SlBWR12* locus co-segregated with resistance to Ral strain GMI1000 in an F_2 population derived from 'HW7996' × 'M82'. All 30 F_1 plants were resistant, and the 83 F_2 individuals segregated 19 R : 41 H : 23 S at the locus (χ^2 = 0.40, P = 0.82), with disease severity differing significantly among the three genotype classes at 15 dpi (Supplementary Fig. 8; Supplementary Table 9). The resistance phenotype observed in all F_1 plants and heterozygous F_2 plants supports a dominant effect of the 'HW7996'-derived resistance allele.

SlBWR12 overexpression restores resistance in susceptible tomato

To determine whether *SlBWR12* is sufficient to confer bacterial wilt resistance, we introduced a constitutive *SlBWR12* overexpression (OE) construct into the susceptible cultivar 'MM'. Transcript analysis by reverse transcriptase-quantitative PCR (RT-qPCR) of independent transgenic lines showed increased *SlBWR12* transcripts in all OE lines compared to empty vector (EV) controls (Fig. 3a). Transgenic tomato lines overexpressing *SlBWR12* and the other three candidate RLP genes showed no obvious developmental abnormalities, and the measured vegetative growth and fruit-related traits did not differ significantly from 'MM'-EV control plants under our experimental conditions (Supplementary Fig. 7c,d). *SlBWR12*-OE lines displayed strong resistance to Ral strain SL1944; there was minimal wilting at 15 dpi and full survival through 20 dpi, comparable to the resistant 'HW7996-EV' (Fig. 3b). The DSI for the *SlBWR12*-OE lines was consistently low and statistically indistinguishable from 'HW7996'-EV controls. In contrast, lines that overexpressed the other three RLP candidate genes were as susceptible as 'MM' (P < 0.05 by repeated-measures ANOVA; P < 0.05, Tukey's HSD at 18 dpi; Fig. 3c). Further, bacterial growth in *SlBWR12*-OE1 plants was inhibited compared with 'MM'-EV from 3 dpi (P < 0.01). At 4 dpi, titers in *SlBWR12*-OE1 (3.0–5.73 × 10^7 CFU cm^{-2}) were significantly lower than the susceptible control but slightly higher than 'HW7996'-EV (Fig.

3d). Additional bacterial population analyses following root and direct stem inoculation showed that disruption of *SlBWR12* increased bacterial proliferation in both root and stem tissues, whereas *SlBWR12* overexpression restricted bacterial growth, indicating that *SlBWR12*-mediated resistance is not limited to the root entry stage but also contributes to restricting bacterial proliferation within stem tissues (Supplementary Fig. 9).

Additionally, to determine whether *SlBWR12* enhanced resistance against multiple RSSC strains, we challenged the OE lines with two additional RSSC strains, SL882 and GMI1000, in addition to SL1944. In all three assays, the wilt rates in *SlBWR12*-OE1 and *SlBWR12*-OE2 were indistinguishable from 'HW7996'. In contrast, OE lines of the other RLP candidate genes were fully susceptible, similar to 'MM'-EV (Fig. 3e). Thus, as *SlBWR12* confers strong resistance to multiple tested bacterial wilt strains in an otherwise susceptible background, it is a major contributor to wilt resistance and a promising genetic resource for improving bacterial wilt resistance in cultivated tomato.

SlBWR12 **mediates bacterial wilt resistance across heterologous hosts**

To further evaluate the contribution of *SlBWR12* to bacterial wilt resistance, we generated stable *SlBWR12*-overexpressing *Nicotiana benthamiana* lines. *SlBWR12* expression in the independent overexpression lines was confirmed by RT-PCR (Supplementary Fig. 10). Among the four *Ralstonia* strains tested in *N. benthamiana,* SL1944 and SL882 were selected for subsequent resistance assays because they reproducibly induced clear wilting symptoms (Supplementary Fig. 11).

Following leaf infiltration with SL1944 and SL882 at different bacterial concentrations, the representative *SlBWR12*-overexpressing T_2 lines OE-1 showed reduced necrotic

symptoms compared with empty vector (EV) plants, particularly at 10^7 CFU mL^{-1} (Fig. 4a). Quantification of lesion area after SL1944 infiltration confirmed a significant reduction in lesion development in the overexpression lines (63.6%) compared with EV plants (87.9%) (Fig. 4b). Consistent with the reduced lesion phenotype, histochemical staining revealed altered defense-associated responses in the *SlBWR12*-overexpressing plants. DAB staining at 3 dpi showed reduced ROS-associated staining, whereas trypan blue staining at 4 dpi revealed markedly reduced cell death at the inoculation sites in OE-1 compared with EV plants following SL1944 inoculation (Fig. 4c). Together, these results do not support the induction of a classical HR-like cell death response by *SlBWR12*; rather, *SlBWR12* overexpression was associated with reduced pathogen-induced lesion development and cell death. RT–qPCR analysis of the defense-related marker genes *Hsr203j*, *Pti5*, *PR4,* and *PR1a* revealed altered temporal expression patterns in *SlBWR12*-overexpressing plants following SL1944 inoculation (Fig. 4d). Thus, *SlBWR12*-mediated resistance is accompanied by defense-associated transcriptional responses despite the absence of pronounced HR-like cell death.

We further assessed bacterial wilt resistance using soil-drench inoculation. Following inoculation with SL1944 at 2×10^6 CFU g^{-1} soil, OE-1 and OE-2 plants displayed markedly reduced wilting symptoms compared with EV plants (Fig. 4e). Disease progression analysis showed significantly lower DSI in both *SlBWR12*-overexpressing lines compared with EV plants (1.5 for OE-1 and 1.2 for OE-2 vs. 3.7 for EV at 20 dpi; Fig. 4f). Consistent with the disease phenotype, bacterial populations were also significantly reduced in the overexpression lines compared with EV plants (Fig. 4g). Together, these results demonstrate that stable overexpression of *SlBWR12* enhances resistance to *R. pseudosolanacearum* in *N. benthamiana* by limiting disease development and bacterial proliferation.

To further evaluate the applicability of *SlBWR12* beyond model systems, we generated *SlBWR12*-overexpressing transgenic potato (*Solanum tuberosum* cv. ‘Desiree’)

lines and challenged them with an *R. syzygii* SL2064 (phylotype IV; potato isolated). Following inoculation, *SlBWR12*-overexpression lines exhibited significantly less severe wilting symptoms than empty vector (EV) control plants, which developed severe wilt by 10 dpi (Fig. 4h). Quantitative DSI values were consistent with these observations, showing that *SlBWR12*-overexpressing plants had significantly lower disease severity indices than EV controls at both 10 dpi (estimate ± s.d. = −1.567 ± 0.099, $P < 0.0001$) and 15 dpi (estimate ± s.d. = −2.608 ± 0.171, $P < 0.0001$) (Fig. 4i). Together, these results demonstrate that *SlBWR12* confers effective bacterial wilt resistance in a susceptible potato background, supporting its functional transferability and potential applicability for cross-crop resistance engineering.

Structural divergence, evolutionary origin, and introgression of *SlBWR12* from wild tomato restores resistance lost during domestication

We compared the predicted protein structures of *SlBWR12* orthologs and variants in resistant vs. susceptible tomato accessions using AlphaFold3[24]. The *SlBWR12* orthologs were identical in all resistant accessions, except for ‘Hawaii7998’, which had a single amino acid substitution compared to the canonical resistant allele (Supplementary Fig. 5b and 12a). In contrast, orthologs from susceptible accessions had markedly reduced similarity, with premature stop codons that truncated the leucine-rich repeat (LRR) domain (Supplementary Figs. 12b–j). Among the susceptible accessions, the cultivated tomato *S. lycopersicum* ‘M82’ and the wild relative *S. pimpinellifolium* ‘LA1589’ showed relatively high overall structural similarity to *SlBWR12* (TM-score ≥ 0.74; Supplementary Fig. 12)

A more detailed structural alignment using FoldMason[25] revealed a lower similarity for the ortholog from ‘M82’, with a local distance difference test (LDDT) score of 0.559, whereas the ortholog from ‘LA1589’ showed a higher similarity (LDDT = 0.904; Supplementary Fig.

13a,b). Sequence comparison based on structural alignment between SlBWR12 in ‘HW7996’ and the ‘LA1589’ ortholog revealed a 23-amino-acid deletion, together with additional local sequence variation within the LRR domain (Supplementary Fig. 13c,d). LRR motif analysis further revealed that the 23-amino-acid deletion encompasses an entire predicted LRR motif, resulting in a single-repeat difference and subtle structural divergence between SlBWR12 and the ‘LA1589’ ortholog (Supplementary Fig. 13e). These results suggest that LRR ectodomain variations distinguish functional SlBWR12 from structurally similar but functionally distinct orthologs.

To trace the evolutionary history of *SlBWR12*, we performed micro-synteny analysis of the chromosome 12 QTL region across 14 tomato accessions, including 10 wild *Solanum* species (Supplementary Table 8). Although the syntenic framework was largely conserved, the RLP cluster flanking *SlBWR12* varied in copy-number and gene-order, ranging from one to four RLP homologs per accession (Fig. 5a). Among these, the syntenic configuration of the *S. lycopersicum* accessions, including ‘HW7996,’ was most like that of the wild species *S. pimpinellifolium* ‘LA1589’, supporting their close evolutionary relationship. Whereas ‘HW7996’ had *SlBWR12* and three additional RLP paralogs arranged in tandem, ‘LA1589’ had a conserved block of three RLPs. In contrast, the reference ‘Heinz1706’ retained only three homologs (*Solyc12g009720*, *Solyc12g009730*, and *Solyc12g009780*). Both *SlBWR12* and hw3740 (*SlyHW12g003740*) corresponded to a single ‘Heinz1706’ ortholog, *Solyc12g009780*, indicating contraction compared to ‘HW7996’ and ‘LA1589’ (Fig. 5a). Thus, domesticated *S. lycopersicum* accessions preserved overall synteny but lost functional resistance alleles through truncation and pseudogenization.

To determine evolutionary relationships, we reconstructed a maximum-likelihood phylogeny of RLPs from the syntenic region, expanding the analysis to include six additional wild accessions for improved phylogenetic resolution (Supplementary Table 10). The

sequences formed four distinct subclades defined by the ‘HW7996’ paralogs (Fig. 5b). Notably, *SlBWR12* from ‘HW7996’ clustered more closely with RLPs of *S. pimpinellifolium* (*SPI12g00577* and *Spim12g009070*) than with cultivated *S. lycopersicum* orthologs (*Solyc12g003850* and *Solyv12g003850*), supporting a model in which *SlBWR12* is derived from introgression from *S. pimpinellifolium* rather than arising de novo in cultivated tomato. Comparison of domain architectures further revealed substantial variation in protein length and domain organization among *SlBWR12* orthologs, with particularly pronounced differences in the length and composition of the LRR region (Fig. 5b). Several orthologs showed truncations or altered LRR configurations, indicating that structural divergence among these RLPs is concentrated largely within the extracellular LRR ectodomain.

Together, these results suggest that *SlBWR12* originated from an ancestral RLP through successive duplication events, followed by lineage-specific functional divergence and retention in *S. pimpinellifolium* (Fig. 5c; Supplementary Table 10). In contrast, cultivated *S. lycopersicum* subsequently lost resistance despite the retention of synteny, likely due to relaxed selection during domestication. Historical introgression from resistant *S. pimpinellifolium* accessions by breeding in the mid-20th century reintroduced a functional *SlBWR12* allele, producing the resistant breeding line ‘HW7996’[18,26].

Discussion

This study resolves a six-decade-old genetic question in tomato by identifying *SlBWR12* as a major-effect resistance gene within the classical *Bwr-12* locus. Loss-of-function substantially reduced resistance, whereas transgenic expression conferred resistance in a susceptible background, demonstrating that this receptor-like protein makes a major contribution to resistance against multiple RSSC strains. To our knowledge, this represents the first cloning of a major-effect QTL gene underlying bacterial wilt resistance in tomato, converting a long-mapped QTL into a defined molecular component.

Our findings position *SlBWR12* as a major-effect RLP-type cell-surface immune receptor that contributes to resistance against multiple tested strains of the *Ralstonia solanacearum* species complex (RSSC). Cell-surface immune receptors, including receptor-like proteins (RLPs), provide an important genetic framework for pathogen perception and have considerable potential for disease-resistance breeding[27,28]. Within the strains and lineages examined here, *SlBWR12* enhanced resistance and restricted bacterial proliferation in susceptible tomato backgrounds, while its activity in *Nicotiana benthamiana* and potato indicates functional compatibility across solanaceous hosts. However, *SlBWR12* alone does not fully recapitulate the resistance phenotype of ‘HW7996’, indicating that its contribution is embedded within a broader quantitative resistance architecture. Consistent with previous genetic studies, additional loci, particularly *Bwr-6*, likely contribute to the magnitude, stability, and strain dependence of resistance; thus, *SlBWR12* is best regarded as a primary major-effect component rather than a single locus sufficient to explain the full resistance phenotype of ‘HW7996’.

Consistent with the general mode of RLP-mediated immunity in plants, the extracellular LRR domain of *SlBWR12* is likely important for receptor function. Comparative

analyses show that resistant accessions preserve an intact and highly conserved LRR ectodomain, whereas susceptible accessions carry deletions or substitutions that disrupt this structural region (Supplementary Figs 10 and 11). These alterations may compromise receptor function, potentially by affecting ligand perception, protein stability, or structural integrity, and thereby contribute to reduced resistance. Together, these observations suggest that conservation of the *SlBWR12* LRR ectodomain is associated with functional *SlBWR12*-mediated resistance and may be important for pathogen perception and subsequent activation of immune responses. Notably, *SlBWR12*-mediated resistance in *N. benthamiana* was not accompanied by enhanced HR-like cell death. Instead, *SlBWR12* overexpression significantly reduced necrotic lesion development, ROS-associated staining, and host cell death, and modulated defense-related gene expression while restricting bacterial proliferation in planta (Fig. 4a–g). Thus, in this heterologous host, effective *SlBWR12*-mediated resistance was associated with pathogen restriction rather than a pronounced macroscopic HR.

Furthermore, SlBWR12-mediated resistance was observed across multiple tested RSSC strains and solanaceous host backgrounds. Within tomato, *SlBWR12* provided effective resistance not only against tomato-derived strains such as GMI1000 (phylotype I; tomato isolate), but also against isolates originating from other solanaceous hosts, including SL882 (phylotype I; eggplant isolate) and SL1944 (phylotype I; tobacco isolate), indicating that its activity is not restricted to host-specific tomato–pathogen interactions (Fig. 2 and 3). Functional transferability was further supported in heterologous solanaceous hosts. Stable expression of *SlBWR12* enhanced resistance to phylotype I *R. pseudosolanacearum* strain SL1944 in *N. benthamiana*, whereas transgenic potato expressing *SlBWR12* showed increased resistance to the potato-derived phylotype IV *R. syzygii* strain SL2064 (Fig. 4). These results demonstrate that *SlBWR12* can function in more than one solanaceous host and that resistance was observed in experimental combinations involving two distinct RSSC

phylotypes. Nevertheless, because phylotype II and III strains were not available and were therefore not tested in the present study, the present data do not establish resistance across the full taxonomic diversity of the RSSC. In particular, activity against phylotype II, including the globally important phylotype IIB-sequevar 1 potato brown-rot lineage, remains to be determined in future investigations.

From an evolutionary perspective, *SlBWR12* belongs to the Cf clade of receptor-like proteins, a lineage shaped by diversification to expand pathogen recognition[29]. Tandem duplication and subsequent diversification are common evolutionary mechanisms underlying the expansion of plant resistance-gene families[30], Our syntenic and phylogenetic analyses are consistent with *SlBWR12* representing an ancestral resistance-associated RLP allele related to sequences retained in wild Solanum lineages, whereas homologous sequences are frequently disrupted or truncated in cultivated tomato accessions. This pattern suggests that functional variation within the *SlBWR12* lineage accompanied the evolutionary and breeding history of tomato, although the selective processes responsible for the present allele distribution remain unresolved. The presence of an intact functional allele in the resistant breeding line ‘HW7996’ therefore highlights wild and breeding germplasm as important reservoirs of immune-receptor diversity that may have been reduced during crop improvement (Fig. 5).

From a translational perspective, the molecular cloning of *SlBWR12* converts a component of the long-mapped *Bwr-12* QTL into a defined molecular target that can complement conventional QTL-based improvement. Sequence-defined functional and disrupted alleles provide a basis for diagnostic markers and gene-based selection, while transgenic or cisgenic deployment and, where technically feasible, precise genome editing or allele replacement could facilitate the deployment of functional *SlBWR12* alleles in susceptible genetic backgrounds. Notably, manipulation of *SlBWR12* did not produce significant changes

in the measured fruit weight or dimensions under our experimental conditions (Supplementary Fig. 7), providing no evidence for a major direct pleiotropic effect on these traits, although linkage to neighboring fruit-related loci cannot be excluded. Its cross-species functionality further suggests potential utility across solanaceous crops, but the durability and spectrum of this resistance will require validation across broader host genetic backgrounds and RSSC diversity[27]. The natural structural variation identified within the LRR ectodomain may also provide a foundation for future receptor engineering once the molecular determinants of recognition are established[31]. Collectively, *SlBWR12* provides a gene-level resource that can be combined with additional resistance loci, including *Bwr-6*, to develop more predictable and durable bacterial wilt resistance within a multi locus framework consistent with the quantitative resistance architecture of ‘HW7996’.

References

1 Elghoul, O. *et al.* Implications for agricultural sustainability: predicting the global distribution of *Ralstonia solanacearum* under current and future climate scenarios. *Front. Plant Sci.* **16**, 1548640 (2025).

2 Álvarez, B., López, M. M. & Biosca, E. G. *Ralstonia solanacearum* facing spread-determining climatic temperatures, sustained starvation, and naturally induced resuscitation of viable but non-culturable cells in environmental water. *Microorganisms* **10**, 2503 (2022).

3 Okiro, L. A., Mulwa, R. M., Oyoo, M. E. & Nyalala, S. The danger of the spread of *Ralstonia solanacearum* on potato crops worldwide and potential mitigation options. *CAB Rev.* **19** (2024). https://doi.org/https://doi.org/10.1079/cabireviews.2024.0014

4 Wang, Z. *et al. Ralstonia solanacearum*–a soil borne hidden enemy of plants: research development in management strategies, their action mechanism and challenges. *Front. Plant Sci.* **14**, 1141902 (2023).

5 Cardenas Gomez, K. *et al.* The epidemiology and management of *Ralstonia solanacearum* and *Ralstonia pseudosolanacearum* in Central and Northern Europe. *Plant Health Cases*, phcs20240028 (2024).

6 Jang, S., Son, J.-S., Schmelz, E. A. & Ryu, C.-M. Novel weapon-aided plant protection in the underground battlefield. *Plant Signaling Behav.* **19**, 2404808 (2024).

7 Nguyen, L. T. T. *et al.* Biological control of tomato bacterial wilt and apple fire blight through the induced resistance of azomycin derived from *Streptomyces* sp. JCK. *Front. Plant Sci.* **16**, 1654826 (2025).

8 Sharma, P. *et al.* Meta-analysis of the *Ralstonia solanacearum* species complex (RSSC) based on comparative evolutionary genomics and reverse ecology. *Microb. Genomics* **8**, 000791 (2022).

9 Balamurugan, A. *et al.* Phylogenetic Diversity and Clonal Expansion in the *Ralstonia solanacearum* Species Complex: A Case Study With Bacterial Wilt Outbreak in Eggplant. *Plant Pathol.* (2025).

10 An, Y. & Zhang, M. Advances in understanding the plant-*Ralstonia solanacearum* interactions: unraveling the dynamics, mechanisms, and implications for crop disease resistance. *New Crops* **1**, 100014 (2024).

11 Qi, P. *et al.* Ubiquitination and degradation of plant helper NLR by the *Ralstonia solanacearum* effector RipV2 overcome tomato bacterial wilt resistance. *Cell Rep.* **43** (2024).

12 Narusaka, M., Hatakeyama, K., Shirasu, K. & Narusaka, Y. *Arabidopsis* dual resistance proteins, both RPS4 and RRS1, are required for resistance to bacterial wilt in transgenic *Brassica* crops. *Plant Signal. Behav.* **9**, e29130 (2014).

13 Godiard, L. *et al.* ERECTA, an LRR receptor-like kinase protein controlling development

pleiotropically affects resistance to bacterial wilt. *Plant J.* **36**, 353–365 (2003).
14 Thomas, N. C. *et al.* The immune receptor Roq1 confers resistance to the bacterial pathogens *Xanthomonas, Pseudomonas syringae*, and *Ralstonia* in tomato. *Front. Plant Sci.* **11**, 463 (2020).
15 Cao, Z. *et al. AhBWR15*, a novel RLK gene, confers resistance to *Ralstonia solanacearum* in peanut. *Plant Biotechnol. J.* **24**, 3861–3875 (2026).
16 Kunwar, S. *et al.* Characterization 3333 of tomato (*Solanum lycopersicum*) accessions for resistance to phylotype I and phylotype II strains of the *Ralstonia solanacearum* species complex under high temperatures. *Plant Breed.* **139**, 389–401 (2020).
17 Wang, J. F., Hanson, P. & Barnes, J. in *Bacterial wilt disease: Molecular and ecological aspects* (eds P Prior, C Allen, & J Elphinstone) 269–275 (Springer, 1998).
18 Scott, J., Wang, J. & Hanson, P. *Breeding tomatoes for resistance to bacterial wilt, a global view.* Vol. 695 (2004).
19 Wang, J. F. *et al.* Identification of major QTLs associated with stable resistance of tomato cultivar 'Hawaii 7996' to *Ralstonia solanacearum*. *Euphytica* **190**, 241–252 (2013).
20 Shin, I. S. *et al.* Construction of a single nucleotide polymorphism marker based QTL map and validation of resistance loci to bacterial wilt caused by *Ralstonia solanacearum* species complex in tomato. *Euphytica* **216**, 54 (2020).
21 Kwon, J. S., Shilpha, J., Lee, J. & Yeom, S.-I. Beyond NGS data sharing for plant ecological resilience and improvement of agronomic traits. *Sci. Data* **11**, 466 (2024).
22 Abebe, A. M. *et al.* Fine mapping and candidate gene analysis of *Bwr-6* conferring bacterial wilt resistance in tomato. *Scientia Horticulturae* **365**, 114964 (2026).
23 Wang, G. *et al.* Resistance against *Ralstonia solanacearum* in tomato depends on the methionine cycle and the γ-aminobutyric acid metabolic pathway. *Plant J.* **97**, 1032–1047 (2019).
24 Abramson, J. *et al.* Accurate structure prediction of biomolecular interactions with AlphaFold 3. *Nature* **630**, 493–500 (2024).
25 Gilchrist, C. L., Mirdita, M. & Steinegger, M. Multiple protein structure alignment at scale with FoldMason. *BioRxiv*, 2024.2008. 2001.606130 (2024). https://doi.org/https://doi.org/10.1101/2024.08.01.606130
26 Thoquet, P. *et al.* Quantitative trait loci determining resistance to bacterial wilt in tomato cultivar Hawaii7996. *Mol. Plant-Microbe Interact.* **9**, 826–836 (1996).
27 Yang, Y. *et al.* Engineered pattern recognition receptors enhance broad-spectrum plant resistance. *Nat. Biotechnol.*, 1–7 (2025).
28 Ngou, B. P. M., Wyler, M., Schmid, M. W., Kadota, Y. & Shirasu, K. Evolutionary trajectory of pattern recognition receptors in plants. *Nat. commun.* **15**, 308 (2024).
29 Kang, W. H. & Yeom, S. I. Genome-wide identification, classification, and expression analysis

of the receptor-like protein family in tomato. *Plant Pathol. J.* **34**, 435 (2018).

30 Li, N. *et al.* Super-pangenome analyses highlight genomic diversity and structural variation across wild and cultivated tomato species. *Nat. Genet.* **55**, 852–860 (2023).

31 Li, T. *et al.* Unlocking expanded flagellin perception through rational receptor engineering. *Nat. plants* **11**, 1628–1641 (2025).

32 Kwak, M. J. *et al.* Rhizosphere microbiome structure alters to enable wilt resistance in tomato. *Nat. Biotechnol.* **36**, 1100–1109 (2018).

33 Koo, H. *et al.* Two long read-based genome assembly and annotation of polyploidy woody plants, Hibiscus syriacus L. using PacBio and Nanopore platforms. *Sci. Data.* **10**, 713 (2023).

34 Marçais, G. & Kingsford, C. A fast, lock-free approach for efficient parallel counting of occurrences of k-mers. *Bioinformatics* **27**, 764–770 (2011).

35 Ranallo-Benavidez, T. R., Jaron, K. S. & Schatz, M. C. GenomeScope 2.0 and Smudgeplot for reference-free profiling of polyploid genomes. *Nature communications* **11**, 1432 (2020).

36 Freire, B., Ladra, S. & Parama, J. R. Memory-efficient assembly using Flye. *IEEE/ACM Trans. Comput. Biol. Bioinf.* **19**, 3564–3577 (2021).

37 Walker, B. J. *et al.* Pilon: an integrated tool for comprehensive microbial variant detection and genome assembly improvement. *PloS one* **9**, e112963 (2014).

38 Alonge, M. *et al.* Automated assembly scaffolding using RagTag elevates a new tomato system for high-throughput genome editing. *Genome Biol.* **23**, 258 (2022).

39 Chen, N. Using Repeat Masker to identify repetitive elements in genomic sequences. *Curr. Protoc. Bioinform.* **5**, 4–10 (2004).

40 Cantarel, B. L. *et al.* MAKER: an easy-to-use annotation pipeline designed for emerging model organism genomes. *Genome Res.* **18**, 188–196 (2008).

41 Salamov, A. A. & Solovyev, V. V. Ab initio gene finding in Drosophila genomic DNA. *Genome Res.* **10**, 516–522 (2000).

42 Kim, S. *et al.* TGFam-Finder: a novel solution for target-gene family annotation in plants. *New Phytol.* **227**, 1568–1581 (2020).

43 Cantalapiedra, C. P., Hernández-Plaza, A., Letunic, I., Bork, P. & Huerta-Cepas, J. eggNOG-mapper v2: Functional Annotation, Orthology Assignments, and Domain Prediction at the Metagenomic Scale. *Mol. Biol. Evol.* **38**, 5825–5829 (2021). https://doi.org/10.1093/molbev/msab293

44 Simao, F. A., Waterhouse, R. M., Ioannidis, P., Kriventseva, E. V. & Zdobnov, E. M. BUSCO: assessing genome assembly and annotation completeness with single-copy orthologs. *Bioinformatics* **31**, 3210–3212 (2015). https://doi.org/10.1093/bioinformatics/btv351

45 Kwon, J. S., Lee, J., Shilpha, J., Jang, H. & Kang, W. H. The landscape of sequence variations between resistant and susceptible hot peppers to predict functional candidate genes against bacterial wilt disease. *BMC Plant Biol.* **24**, 1036 (2024).

46 Ma, X. *et al.* The spinach YY genome reveals sex chromosome evolution, domestication, and introgression history of the species. *Genome Biol.* **23**, 75 (2022).

47 Chen, T. *et al.* Landscape genomics reveals adaptive genetic differentiation driven by multiple environmental variables in naked barley on the Qinghai-Tibetan Plateau. *Heredity* **131**, 316–326 (2023).

48 Lee, J., Jang, H., Kang, W.-H. & Yeom, S.-I. Transcriptome analysis of pepper-*Phytophthora infestans* interaction based on a pipeline of a simplified and effective RNA-seq analysis (PoRAS). *Hortic. Sci. Technol.* **41**, 100–110 (2023).

49 Weber, E., Engler, C., Gruetzner, R., Werner, S. & Marillonnet, S. A modular cloning system for standardized assembly of multigene constructs. *PloS One* **6**, e16765 (2011).

50 Jeong, J. h., Jeon, E.-y., Hwang, M. K., Song, Y. J. & Kim, J.-Y. Development of super-infective ternary vector systems for enhancing the *Agrobacterium*-mediated plant transformation and genome editing efficiency. *Hortic. Res.* **11**, uhae187 (2024).

51 Waterhouse, A. M., Procter, J. B., Martin, D. M., Clamp, M. & Barton, G. J. Jalview Version 2—a multiple sequence alignment editor and analysis workbench. *Bioinformatics* **25**, 1189–1191 (2009).

52 Yoo, H. J. *et al.* Natural overexpression of *CAROTENOID CLEAVAGE DIOXYGENASE 4* in tomato alters carotenoid flux. *Plant Physiol.* **192**, 1289–1306 (2023).

53 Čermák, T., Baltes, N. J., Čegan, R., Zhang, Y. & Voytas, D. F. High-frequency, precise modification of the tomato genome. *Genome Biol.* **16**, 232 (2015).

54 Lee, H. J., Jo, E.-J., Kim, N.-H., Chae, Y. & Lee, S.-W. Disease responses of tomato pure lines against *Ralstonia solanacearum* strains from Korea and susceptibility at high temperature. *Res. Plant Dis.* **17**, 326–333 (2011).

55 Cho, H. *et al.* Prediction of host-specific genes by pan-genome analyses of the Korean Ralstonia solanacearum species complex. *Frontiers in Microbiology* **10**, 506 (2019).

56 Cellier, G., Gauche, M. M., Cheron, J. J. & Pecrix, Y. How to conduct phylogenetic endoglucanase (egl) inference using the reference *Ralstonia solanacearum* species complex curated database. *Phytopathology®* **115**, 548–554 (2025).

57 Bittrich, S., Segura, J., Duarte, J. M., Burley, S. K. & Rose, Y. RCSB protein Data Bank: exploring protein 3D similarities via comprehensive structural alignments. *Bioinformatics* **40**, btae370 (2024).

58 Martin, E. C. *et al.* LRRpredictor—a new LRR motif detection method for irregular motifs of plant NLR proteins using an ensemble of classifiers. *Genes* **11**, 286 (2020).

59 Tang, H. *et al.* JCVI: A versatile toolkit for comparative genomics analysis. *iMeta* **3**, e211 (2024).

60 Jones, P. *et al.* InterProScan 5: genome-scale protein function classification. *Bioinformatics* **30**, 1236–1240 (2014).

61 Albert, I. *et al.* An RLP23–SOBIR1–BAK1 complex mediates NLP-triggered immunity. *Nat. plants* **1**, 1–9 (2015).

62 Katoh, K., Misawa, K., Kuma, K. i. & Miyata, T. MAFFT: a novel method for rapid multiple sequence alignment based on fast Fourier transform. *Nucleic Acids Res.* **30**, 3059–3066 (2002).

63 Capella-Gutiérrez, S., Silla-Martínez, J. M. & Gabaldón, T. trimAl: a tool for automated alignment trimming in large-scale phylogenetic analyses. *Bioinformatics* **25**, 1972–1973 (2009).

64 Nguyen, L. T., Schmidt, H. A., Von Haeseler, A. & Minh, B. Q. IQ-TREE: a fast and effective stochastic algorithm for estimating maximum-likelihood phylogenies. *Mol. Biol. Evol.* **32**, 268–274 (2015).

65 Qiao, X. *et al.* Gene duplication and evolution in recurring polyploidization–diploidization cycles in plants. *Genome Biol.* **20**, 38 (2019).

Methods

Plant materials and growth conditions

The *S. lycopersicum* accessions ‘Hawaii7996’ (‘HW7996) and ‘Moneymaker’ (‘MM’) were used as resistant and susceptible controls[32], respectively**.** Transgenic experiments were conducted using ‘HW7996’ and ‘MM’. Transgenic plants were grown in a greenhouse at Gyeongsang National University (35°15′N, 128°10′E; Jinju, Republic of Korea) during the spring seasons of 2022 and 2023 for seed collection. To investigate the inheritance of *Bwr-12* mediated resistance, we used a previously established F_5 recombinant inbred line (RIL) population derived from a cross between ‘HW7996’ and the susceptible *S. lycopersicum* line ‘E6203’[22], alongside an F_2 population generated in this study by crossing ‘HW7996’ with the susceptible cultivar ‘M82’. Plants were maintained under standard greenhouse conditions with adequate irrigation and fertilization, and diseased individuals were removed immediately. For controlled experiments, plants were cultivated in a growth chamber under a 16/8 h light/dark photoperiod at 23–25 °C, whereas plants inoculated with *R. pseudosolanacearum* (Ral) were maintained at 30 °C. Leaves of tomato and *Nicotiana benthamiana* were harvested, frozen immediately in liquid nitrogen, homogenized using a cryogenic grinder, and stored at −80 °C until further analysis.

Sequencing and data preparation

Genomic DNA for long-read sequencing was extracted from young leaves of *S. lycopersicum* ‘HW7996’ using the high-molecular-weight genomic DNA extraction method[33]. Oxford Nanopore long-read libraries were prepared and sequenced on the PromethION platform. Hi-C libraries were generated from cross-linked chromatin following the Dovetail standard protocol using the HindIII-HF restriction enzyme (New England BioLabs), and the resulting

libraries were sequenced on the Illumina NovaSeq 6000 platform to produce 2 × 150 bp paired-end reads. For short-read data used in the 'HW7996' assembly and resequencing analyses, genomic DNA from *S. lycopersicum* 'HW7996' and 'Hawaii7997' was extracted from young leaves using a modified cetyltrimethylammonium bromide (CTAB) method. Paired-end libraries were constructed and sequenced on the Illumina NovaSeq 6000 platform. Previously published whole-genome resequencing datasets for additional tomato accessions were retrieved from public repositories and integrated into the comparative analyses (Supplementary Table 1).

Genome assembly and annotation of 'Hawaii7996'

To assess genome characteristics prior to assembly, a 19-mer frequency distribution was computed from Illumina short reads using Jellyfish v2.3.0[34], and genome size, heterozygosity, and repeat content were estimated with GenomeScope 2.0[35]. De novo assembly was performed with Flye v2.5[36] and subsequently polished in three iterative rounds using Pilon v1.21[37] with high-quality Illumina paired-end reads to correct base-level errors and small indels. Hi-C reads were processed with Juicer and 3D-DNA for chromosome scaffolding, and final pseudomolecules were anchored and ordered relative to the tomato reference genome (ITAG4.0) using RagTag v2.1.0[38].

Repetitive elements were annotated with RepeatMasker v4.1.5[39] using a custom library generated by RepeatModeler v2.0.5. Gene prediction was carried out using MAKER v3.01.03[40], integrating ab initio models (SNAP and AUGUSTUS), homology-based evidence from the *S. lycopersicum* 'Heinz 1706' genome, and transcript evidence derived from 'HW7996' RNA-seq data. For improved model sensitivity, annotations were filtered using an annotation edit distance (AED) threshold of ≤ 1.

To refine gene models within the *Bwr-12* QTL interval, additional re-annotation was performed with Fgenesh[41] and TGFam-Finder[42], supported by Pfam domain searches. Final gene sets were curated and formatted with AGAT (v1.4.0; [https://www.doi.org/10.5281/zenodo.3552717]) and functionally annotated using multiple databases, including NR, eggNOG, GO, KEGG, TrEMBL, KOG, SWISS-PROT, and Pfam[43]. Assembly completeness was evaluated using BUSCO v5.0.0 (eukaryota_odb10)[44], and overall quality metrics were further assessed through alignment-based statistics.

Genome-wide variant identification based on the 'Hawaii7996' reference

Variant identification was performed for seven resistant and 11 susceptible tomato accessions following previously described methods[45]. The resequencing panel was selected as a phenotype-contrasting set of accessions with documented bacterial wilt resistance or susceptibility and available whole-genome sequencing data, rather than to represent population-wide genetic diversity in tomato. Detailed information on the species, genetic background, geographic origin, bacterial wilt phenotype, *Ralstonia* strains used for phenotypic evaluation, and corresponding references for all 19 accessions, including 'HW7996', is provided in Supplementary Table 11. Raw Illumina reads from all resequencing datasets were trimmed to remove adapters and low-quality bases (Phred < 20) using Trimmomatic v0.39 and Cutadapt v1.18. Clean reads were aligned to the 'HW7996' reference genome using BWA-MEM v0.7.17, and duplicate reads were marked with Picard v3.0.0. Variants were called following the GATK v4.4.0.0 Practices pipeline (HaplotypeCaller and GenotypeGVCFs) with QUAL < 30, DP < 10, and GQ < 20. The numbers of SNPs and InDels within 1-Mb genomic windows were counted to construct a genome-wide map of variant density. Large-scale structural variants (> 50 bp) were identified with Assemblytics (v1.2; [http://assemblytics.com/]; accessed 2025.11.10). Genome-wide variant distributions were visualized with Circos[45].

Identification of candidate QTL regions and genes associated with bacterial wilt resistance

Identification of BW resistance candidate genes based on SNP variations between resistant and susceptible accessions was performed using resequencing data aligned to the resistant reference genome 'HW7996'. The analysis followed the workflow shown in Supplementary Fig. 14, and detailed procedures are described below. Nine previously reported markers from Chr6 and Chr12 (Supplementary Table 3) were mapped to the 'HW7996' assembly by BLASTn (identity > 90% and query coverage > 80%) (Fig. 1a). Based on the marker intervals defined for each QTL region, SNPs were extracted from the variant calling results of individual resequencing datasets to identify reference-relative variants in resistant and susceptible accessions. To compare sequence variation between resistant and susceptible tomato accessions, SNPs within the QTL marker intervals were extracted and binarized as different (0) or identical (1) to the reference genome. Based on these criteria, an SNP matrix for all accessions was constructed (Supplementary Tables 4 and 7).

The variant conservation rate (VCR) was calculated using a sliding-window approach. To evaluate the effect of window size on candidate-region localization on chromosome 12, ΔVCR profiles were compared using three window/step combinations: 200 kb/40 kb, 100 kb/20 kb, and 50 kb/10 kb. The 100-kb/20-kb and 50-kb/10-kb settings localized the major ΔVCR signal to the same candidate region, whereas the 200-kb/40-kb setting produced a broader profile with a partially shifted peak maximum, consistent with reduced positional resolution at the larger window size. We therefore selected the 100-kb window with a 20-kb step for chromosome 12 as an intermediate setting that balanced local signal smoothing and spatial resolution. For the *Bwr-6* region on chromosome 6, a 100-kb window with a 10-kb step was used, whereas a 10-kb window with a 2-kb step was applied for whole-chromosome

visualization. Comparable overlapping sliding-window approaches have been used in plant genomic analyses[46,47]. Mean VCRs for resistant and susceptible groups were then compared to identify genomic regions (ΔVCR). By design, ΔVCR $\in$ [−1, 1]: positive values indicate more SNPs (greater divergence from 'Hawaii7996') in the susceptible group, negative values indicate more SNPs in the resistant group (Fig. 1b).

For the F_5 RILs, genomic DNA was extracted from young leaves using a modified CTAB method. Genotyping was performed using PCR-based InDel and CAPS markers spanning the *Bwr-12* region. Marker names denote the marker type and physical position (bp) in the reference genome, and the corresponding primer sequences and restriction enzymes are provided in Supplementary Table 3. Marker positions and recombination breakpoints were mapped on the 'HW7996' genome using BLASTn. For phenotypic classification, recombinant lines were classified as resistant or susceptible based on whether their plant-level DSI was significantly lower than that of 'E6203' or higher than that of 'HW7996', respectively (one-tailed Student's t-tests, $\alpha = 0.05$). Accordingly, *Bwr-12* was delimited to the 'HW7996'-derived interval shared by all resistant lines but absent from all susceptible lines.

RNA-seq analysis

RNA-seq data were obtained from the NCBI Sequence Read Archive (SRA) (accession: PRJNA493976), which includes root and stem tissues collected at 0, 3, and 5 dpi from resistant and susceptible tomato accessions inoculated with *Ralstonia* RsH[23]. Transcriptome analysis was performed based on a previously reported analysis pipeline[48]. Raw reads were subjected to adapter removal and quality trimming with Trimmomatic v0.39 and Cutadapt v1.18. Clean reads were aligned to the 'HW7996' reference genome using HISAT2 v2.1.0, and feature-level quantification was performed with an in-house script[48] based on gene annotation

of each species.

Gene expression levels were normalized as fragments per kilobase of transcript per million mapped reads (FPKM), and a z-score transformation was applied across samples to standardize gene expression profiles. Differentially expressed genes (DEGs) were identified using the DESeq2 package in R. Genes with an adjusted *P*-value (FDR) < 0.05 and an $|\log_2$ fold change| > 1 were considered significantly differentially expressed. These standardized values were used to construct heatmaps and identify genes exhibiting consistent differential expression between resistant and susceptible interactions. Visualization used the ComplexHeatmap package in R. The domain architecture of candidate genes was analyzed using SMART (v10; [https://smart.embl.de/]), and signal peptide and transmembrane regions were predicted using Phobius (v1.01; [https://phobius.sbc.su.se/]).

CRISPR-Cas9-mediated genome editing

To validate the functional roles of candidate genes within the *Bwr-12* locus, CRISPR–Cas9-mediated mutagenesis was performed in the resistant breeding line ‘HW7996’. Dual guide RNA (gRNA) cassettes were designed for each of the four candidate genes (*SlyHW12g003710*, *SlyHW12g003720*, *SlyHW12g003730*, and *SlyHW12g003740*) using the ‘Hawaii7996’ genome to minimize off-target effects. Candidate gRNA sequences were screened through in-house alignment pipelines and verified manually. Each gRNA pair was cloned into the binary vector pAGM4723, containing a codon-optimized Cas9 driven by the CaMV 35S promoter and an *Arabidopsis U6* (AtU6) promoter for gRNA expression[49]. Constructs were introduced into *Agrobacterium tumefaciens* strain EHA105 harboring a super-ternary helper plasmid (Nulla Bio Inc., Korea)[50] and subsequently transformed into ‘HW7996*’.*

Genomic DNA was extracted using the GeneAll Plant SV kit (GeneAll Biotechnology,

Seoul, Republic of Korea), and successful transformants were verified by PCR and Sanger sequencing. Homozygous T_2 and T_3 lines lacking T-DNA integration were used for all downstream phenotypic and molecular analyses. gRNA sequences and genotyping primers are listed in Supplementary Table 12. Edited alleles were aligned and visualized using MUSCLE (v.2.11.5.0) with default parameters, implemented in Jalview[51].

Construction of overexpression transgenic plants

To evaluate whether the candidate genes for bacterial wilt resistance, full-length coding sequences of *SlyHW12g003710*, *SlyHW12g003720*, *SlyHW12g003730* (*SlBWR12*), and *SlyHW12g003740* were cloned from 'HW7996' cDNA into the pCAMBIA2300 (pC2300) binary vector under the CaMV 35S promoter using a ligation-independent cloning strategy[52]. All constructs were verified by sequencing and introduced into *Agrobacterium tumefaciens* strain EHA105 carrying a super-ternary helper vector (Nulla Bio Inc., Jinju, Republic of Korea).

For transformation, overexpression constructs were introduced into *S. lycopersicum* 'MM' via *Agrobacterium*-mediated transformation of cotyledon explants[53]. Regenerated T_0 plants were acclimatized in soil under controlled growth chamber conditions. Transgene integration was verified by PCR using vector-specific primers, and expression was confirmed by RT-PCR and RT-qPCR, with expression normalized to *SlUBQ*.

For *N. benthamiana* and potato transformation, the pC2300 binary empty vector (EV) control and the *SlBWR12* overexpression construct were introduced via *Agrobacterium tumefaciens* strain GV3101-mediated transformation. Transgenic plants were selected on kanamycin-containing medium, regenerated into whole plants, and acclimatized in soil. Transgene integration was verified by PCR using pC2300 vector-specific primers. For *N. benthamiana*, independent transgenic lines were advanced to the T_2 generation, and

SlBWR12 expression was confirmed by RT-PCR using *NbActin* as the reference gene (Supplementary Fig. 10a). In potato (*Solanum tuberosum* cv. 'Desiree'), T_0 transgenic lines were used for subsequent analyses, and *SlBWR12* expression was likewise confirmed by RT-PCR using *StEF1α* as the reference gene (Supplementary Fig. 10b). All primer information is provided in Supplementary Table 12.

Development and genotyping of the F_1 and F_2 segregating populations

The F_1, F_2, and parental plants ('HW7996' and 'M82) were grown under the growth chamber conditions described above. Genomic DNA was extracted from young leaves using the GeneAll Plant SV kit (GeneAll Biotechnology, Seoul, Republic of Korea). The *SlBWR12* locus was genotyped with a co-dominant deletion marker spanning the structural variation that distinguishes the two parental alleles, amplifying a 1,568 bp product from the 'HW7996' allele and a 1,343 bp product from the 'M82' allele. Amplicons were separated on a 1.5% agarose gel; individuals showing only the 1,568 bp band were scored as homozygous resistant (R), those showing only the 1,343 bp band as homozygous susceptible (S), and those showing both bands as heterozygous (H). Segregation was tested against the expected 1:2:1 ratio by chi-square analysis. Genotyped plants were inoculated with *R. pseudosolanacearum* GMI1000 and scored for DSI as described above. Genotype classes were compared by one-way ANOVA followed by Tukey's HSD test ($P < 0.05$) on individual DSI values at 15 dpi. Marker primer sequences are listed in Supplementary Table 12.

Bacterial inoculation assay

Tomato genome-edited (GE; T_3 generation) and overexpression (OE; T_2 generation) lines were evaluated for resistance against three *Ralstonia* strains: *R. pseudosolanacearum* (Ral)

GMI1000 (phylotype I; tomato isolate), Ral SL1944 (phylotype I; tobacco isolate), and Ral SL882 (phylotype I; eggplant isolate)[54]. Bacteria were cultured on Kelman's TZC medium and subsequently grown in CPG broth at 28 °C. Suspensions were adjusted to 1 × 10^8 CFU mL^{-1} (OD_{600} = 0.3) and applied to soil at 1 × 10^6 CFU g^{-1}.

In parallel with the transgenic assays, the F_1 (30 plants), F_2 (83 plants), and the parental 'HW7996' (14 plants) and 'M82' (10 plants) were inoculated with Ral strain GMI1000 by soil drenching as described above, and the DSI was scored on a 0-4 scale at 15 dpi. The F_5 RILs and their parents were evaluated independently as described previously[22]. Four-week-old seedlings of F_5 RILs were inoculated by dipping the intact root ball for 1 min in a suspension of Ral strain SL882 adjusted to approximately 1 × 10^8 CFU mL^{-1} (OD_{600} = 0.1) and scored on the same 0-4 DSI scale four weeks after inoculation, with at least ten plants per line in three independent experiments.

For *N. benthamiana* resistance assays, transgenic lines (T_2 generation) and empty-vector control plants were inoculated with Ral SL1944 via soil-drenching. Bacterial suspensions prepared as described above were adjusted to 2 × 10^6 CFU mL^{-1} and drenched into the soil of 4-week-old plants. Inoculated plants were incubated in a growth chamber at 28 °C under a 16-hour light/8-hour dark cycle, and wilting symptoms were scored daily over 20 days post-inoculation. To evaluate leaf-specific phenotypes, leaves of 4-week-old *N. benthamiana* plants were infiltrated with Ral SL1944 and SL882. Bacterial suspensions (1 × 10^8, 1 × 10^7, and 1 × 10^6 CFU mL^{-1}) were infiltrated into localized area (approximately 1 cm in diameter) using needleless syringe, and phenotype responses were monitored. All experiments were independently performed three times with similar results.

For potato resistance assays, independent T_0 transformants and control plants were challenged with a RSSC strain, *R. syzygii* SL2064 (phylotype IV; potato isolate)[55]. Bacteria were grown and prepared as described above, and cell suspensions were adjusted to a final

concentration of 1×10^8 CFU mL^{-1}. Stem inoculation was performed by delivering 5 µL of the bacterial suspension directly into the stem, corresponding to an estimated inoculum of approximately 5×10^5 CFU per plant. Inoculated plants were maintained under controlled conditions (30 °C, 16 hours light/8 hours dark), and disease progression was monitored daily for 20 days post-inoculation. Detailed information on the current taxonomic classification, phylotype, biovar, geographic origin, and host of isolation of all *Ralstonia* strains used in this study is provided in Supplementary Table 13. The sequevar of *R. syzygii* strain SL2064 was determined by phylogenetic analysis of its publicly available endoglucanase (*egl*) gene sequence (GenBank accession KY313646.1) using the curated reference dataset[56].

Bacteria colony quantification

For bacterial quantification in tomato, about 100 µL of a Ral strain GMI1000 suspension (gentamicin-resistant, 1×10^4 CFU mL^{-1}) was infiltrated into the third and fourth terminal leaflet of each plant using a needleless syringe. Leaf discs (0.5 cm in diameter) for each designated time point were pooled into 1.5 mL microcentrifuge tubes containing 1 mL of sterile water. Each tube contained four discs of a single plant, representing one biological replicate. Samples were homogenized thoroughly, serially diluted, and plated for bacterial enumeration. Colony counts were converted to log(CFU cm^{-2}). Each treatment included three biological replicates per experiment.

In the case of *N. benthamiana*, the entire leaf surface was infiltrated with Ral SL1944 suspension (1×10^4 CFU mL^{-1}) using a needleless syringe. Four leaf discs (1 cm in diameter) were harvested per plant at 0, 2, 4, and 6 dpi to serve as one biological replicate. All collected samples were thoroughly homogenized, serially diluted, and plated for bacterial enumeration. Colony counts were converted to log(CFU cm^{-2}). Each treatment included four biological

replicates per experiment.

Disease evaluation and data analysis

Disease symptoms were evaluated daily following inoculation with *Ralstonia*. The DSI was scored on a 0–4 scale: 0, no visible wilting; 1, < 25% wilted; 2, 26–50% wilted; 3, 51–75% wilted; and 4, > 76% wilted or dead. The mean DSI and wilt rate (%) were calculated for each genotype. Each biological replicate comprised 20–26 plants, and all experiments were performed in three independent replicates. Statistical analyses were conducted using repeated-measures ANOVA followed by Tukey's HSD test ($P < 0.05$) in R (v4.1). Linear mixed-effects model (LMM) were fitted in R using the lme4 (v.1.1.37) package.

Defense quantification in *Nicotiana benthamiana*

To evaluate defense activation, infiltrated leaves expressing *SlBWR12* or EV were harvested at 0, 3, 6, 12, 24, and 48-hours post-inoculation. Total RNA was isolated with TRIzol (Thermo Fisher Scientific, Waltham, MA, USA), and first-strand cDNA was synthesized from 2 μg of total RNA using oligo(dT) primers and Superscript IV reverse transcriptase (Invitrogen, Carlsbad, CA, USA). RT-qPCR was performed with SYBR Green Master Mix (Qiagen, Hilden, Germany) and gene-specific primers for defense marker genes (*NbHSR203J*, *NPti5*, *NbPR4* and *NbPR1a*). Expression was normalized to *NbActin*. Relative transcript levels were calculated using the $2^{-\Delta\Delta Ct}$ method, and primer efficiencies are provided in Supplementary Table 14.

DAB and Trypan Blue staining

For hydrogen peroxide detection, leaf discs were placed in DAB staining solution [50 mg DAB, 90 mL sterile H_2O, 10 mL 10× phosphate-buffered saline (Solarbio), 25 µL Tween 20 (Solarbio), pH 3.0] at a volume of 3 mL per disc. Samples were vacuum-infiltrated at 0.6 MPa for 2 min and subsequently incubated in the dark at 25 °C for 15 min. Decolorization was performed using 90% ethanol until chlorophyll was completely removed.

For cell death visualization, leaf discs were treated with 3 mL of 0.1% (w/v) Trypan Blue solution (Sigma-Aldrich) per disc. Samples were subjected to two cycles of vacuum infiltration at 0.6 MPa for 5 min with a brief release of vacuum between cycles, followed by incubation at 25 °C for 1 h. Stained samples were destained in 90% ethanol with gentle shaking until leaves were fully cleared. The leaves of ROS accumulation and cell death were observed under a stereomicroscope.

Comparative sequence and structural analysis of *SlBWR12* orthologs and allelic variants

Protein sequences corresponding to *SlBWR12* orthologs and allelic variants were obtained from two sources: resequencing-derived variants generated in this study (‘Hawaii7998’, ‘Alisa craig’, ‘BWS-3’, ‘Gold Nugget’, ‘Moneymaker’, and ‘New Yorker’) and publicly available genome annotations (‘M82’, ‘Heinz1706’, ‘Sweet100’, and ‘LA1589’). Protein structures were predicted using AlphaFold3[24] with default settings, and the top-ranked model for each accession was selected for downstream analyses. Pairwise structural similarity analyses were evaluated using the TM-align algorithm implemented in the RCSB Protein Data Bank[57]. To assess sequence variation in the context of three-dimensional structure, structure-guided alignments were performed using FoldMason[25], focusing in particular on comparison between the ‘M82’ and ‘LA1589’ *SlBWR12* proteins. Structural and sequence alignments generated by

FoldMason were subsequently visualized and annotated using Jalview[51]. LRR motifs in *SlBWR12* and the 'LA1589' ortholog were predicted using LRRpredictor v1.0 web server, and the predicted repeat organization was compared to assess differences in LRR motif number and position within the deletion-containing region[58].

Local synteny and phylogenetic tree analyses of RLPs

To examine the local synteny of the functional RLP-containing region, we performed pairwise synteny analyses between the 'HW7996' genome and 19 tomato genomes, including wild relatives using MCScan implemented in the JCVI package, with default parameters except for the LAST alignment (-a 10 and -b 6)[59]. The syntenic region between two genes (*SlyHW12g003550* to *SlyHW12g003760*) on chromosome 12 of the 'HW7996' genome was selected and visualized. All genes within the syntenic region were extracted, and their protein domains were identified using InterProScan v106.0[60]. The genome assemblies and annotation resources used for the phylogenetic tree analyses summarized in Supplementary Table 15. To obtain orthologs of the four 'HW7996' RLP genes in *Solanum pimpinellifolium*, protein-to-genome mapping was performed using Exonerate (v2.4.0; https://github.com/nathanweeks/exonerate). Based on these results, a protein-based genomic re-annotation was conducted, and the corresponding genes were assigned as *SlyHW12g003710.1-like*, *SlyHW12g003720.1-like*, *SlBWR12-like*, and *SlyHW12g003740.1-like*, respectively.

Genes containing both transmembrane (TM) helices and LRR domains were considered RLP candidates and were marked specifically on the synteny plots. To infer the evolutionary relationship, predicted RLP candidates were selected for phylogenetic analysis. *RLP23* from *Arabidopsis thaliana* was the outgroup[61]. Protein sequences were aligned using MAFFT v7.520 with --maxiterate 1000 and --globalpair options[62]. Positions containing gaps in

more than 20% of the sequences were subsequently trimmed using trimAl v1.4.rev15 with the -gt 0.2 parameter[63]. The best-fit substitution model, JTT+F+I+R3, was selected by ModelFinder implemented in IQ-TREE[64]. A maximum-likelihood phylogenetic tree was then reconstructed using IQ-TREE v2.3.6 with the --B 1000 --alrt 1000 --safe parameters. Duplication patterns were analyzed using DupGen_finder-unique[65].

Data availability

All the data generated in this study have been uploaded to Figshare (https://figshare.com/s/8f1963339a6a05ed465a). The data have been integrated into the 'Hawaii7996' genome annotation information. Detailed information can be found in the Figshare description. Raw sequencing data are available in the NCBI SRA under the BioProject accession number PRJNA1354899.

Acknowledgements

This work was supported by the National Research Foundation of Korea (NRF) grant funded by the Korean government (MSIT) (RS-2023-NR076376, RS-2024-00338092, and RS-2026-25509744). We are grateful to Mr. Hagki Jang for his technical support.

Author contributions

W.-H.K. and S.-I.Y. conceived, designed, and coordinated the project. S.I., B.P., and J.-S.K. performed the experiments. J.H., Junseok L., Y.-M.K, M.-S.K., and J.L. performed bioinformatic analyses. B.P., J.-H.J., H.-Y.L., J.M.L., C.-S.O., J.H.Y., H.-S.K., and J.-S.K. generated the materials used in this study. J.-S.K., J.L., M.-S.K., W.-H.K., and S.-I.Y. wrote the manuscript. J.-S.K., J.L., M.-S.K., S.-W.L, W.-H.K. and S.-I.Y. revised the paper. All authors read and approved the final manuscript.

Competing interests

The authors declare that a patent application related to the findings reported in this study is in preparation. The authors declare no other competing interests.

Additional information

Supplementary information is available for this paper.

Table 1. Genome assembly statistics.

Characteristics by category	HW7996
Assembly statistics	
Number of scaffolds	13
Total length (Mbp)	819.6
Max. scaffolds length (Mbp)	94.7
Average scaffolds length (Mbp)	63.0
N50 (Mbp)	66.6
L50	6
Annotated protein-coding genes	35,909
BUSCO coverage (genome)	
Complete genes (%)	5,852 (98.3%)
Fragmented genes (%)	13 (0.2%)
Missing genes (%)	85 (1.5%)
BUSCO coverage (gene model)	
Complete genes (%)	5,506 (92.5%)
Fragmented genes (%)	65 (1.1%)
Missing genes (%)	379 (6.4%)
Functional annotation	
NCBI NR	30,223 (97.8%)
KEGG	13,065 (42.3%)
GO	12,704 (41.1%)
Swiss-Prot	27,550 (89.1%)
Unannotated	686 (2.2%)
Total	30,909 (100%)

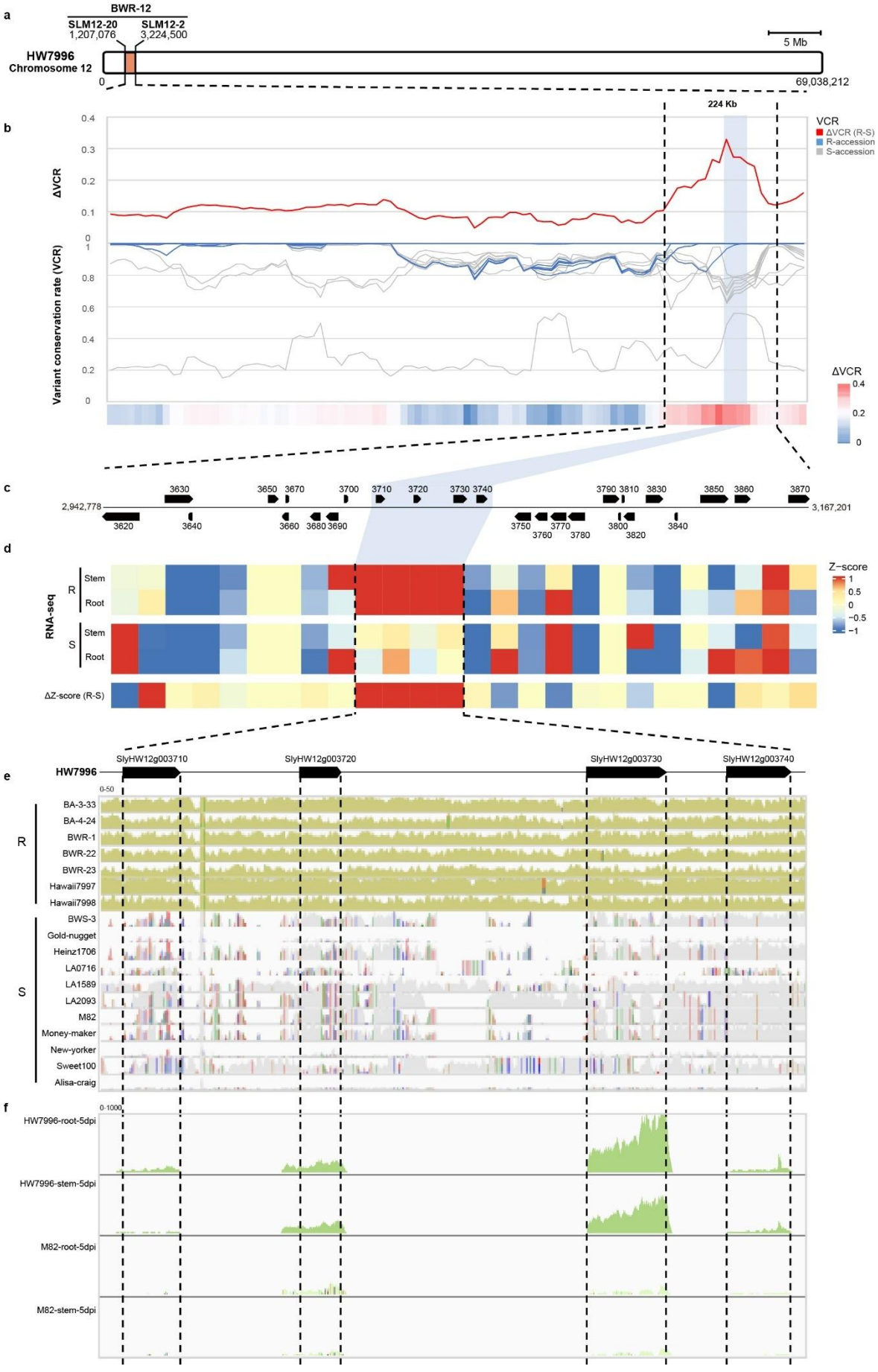

a
BWR-12
SLM12-20
1,207,076
SLM12-2
3,224,500
5 Mb
HW7996
Chromosome 12
0
69,038,212
b
224 Kb
VCR
ΔVCR (R-S)
R-accession
S-accession
ΔVCR
Variant conservation rate (VCR)
c
2,942,778
3,167,201
d
RNA-seq
R
S
Stem
Root
ΔZ-score (R-S)
Z−score
e
HW7996
SlyHW12g003710
SlyHW12g003720
SlyHW12g003730
SlyHW12g003740
BA-3-33
BA-4-24
BWR-1
BWR-22
BWR-23
Hawaii7997
Hawaii7998
BWS-3
Gold-nugget
Heinz1706
LA0716
LA1589
LA2093
M82
Money-maker
New-yorker
Sweet100
Alisa-craig
f
HW7996-root-5dpi
HW7996-stem-5dpi
M82-root-5dpi
M82-stem-5dpi

Figure 1. Dissection of the chromosome 12 QTL region and identification of four candidate genes for bacterial wilt resistance in tomato. a, The *Bwr-12* QTL interval mapped on chromosome 12 of 'HW7996'. The orange-shaded box indicates the *Bwr-12* QTL interval delimited by flanking markers SLM12-20 (1,207,076 bp) and SLM12-2 (3,224,500 bp). The scale bar represents 5 Mb. **b**, Variant conservation density across the QTL region based on whole-genome resequencing. Variant frequencies were calculated using a 100-kb sliding window with a 20-kb step. Gray and blue lines represent susceptible and resistant accessions, respectively; the red line indicates the relative increase in variant density in resistance compared with susceptible accessions. The heatmap below shows the corresponding variant intensity. **c**, Gene location within the refined QTL interval. Arrow orientation indicates transcriptional direction. Gene IDs such as *SlyHW12g003620* are abbreviated by omitting the "SlyHW12g" prefix (for example, "3620"). **d**, Expression patterns of the genes shown in **c**, presented as z-scores. ΔZ-score represents the difference between the mean z-scores of root and stem tissues in resistant versus susceptible groups. **e**, The four genes with the strongest infection-responsive expression in **d** are marked by black bars. The panel below shows IGV read-mapping profiles from resequencing data (scaled to a maximum depth of 50). Yellow and gray indicate resistant and susceptible accessions, respectively. **f**, IGV read-mapping profiles from RNA-seq data (scaled to a maximum depth of 1,000). Samples include root and stem tissues of 'HW7996' and the susceptible 'M82' at 5 days post-inoculation (dpi) with *Ralstonia* strain RsH.

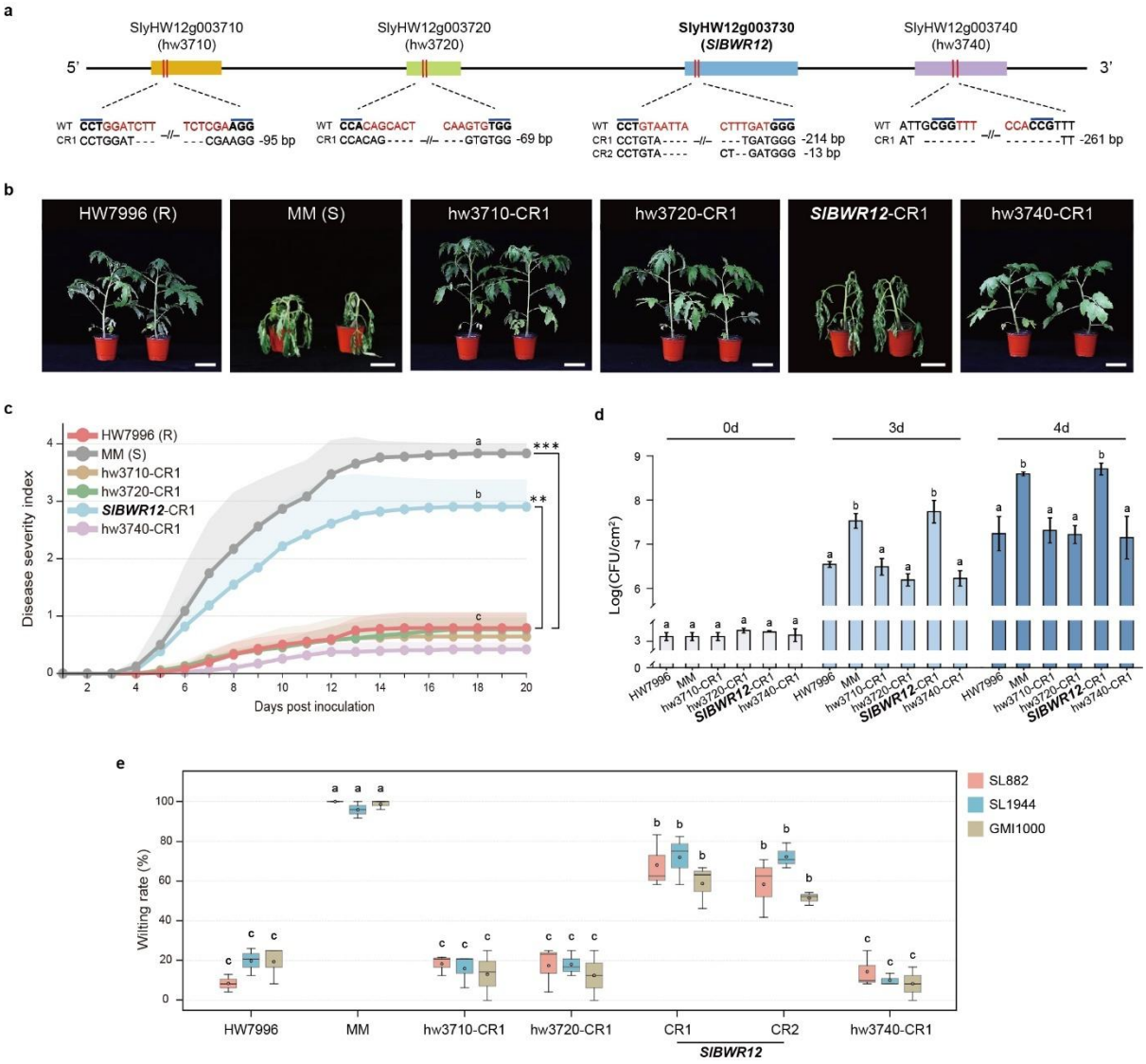


Figure 2. Functional analysis of four candidate genes for bacterial wilt resistance using CRISPR-Cas9. a, CRISPR-Cas9 mutagenesis of four RLP genes (hw3710, hw3720, *SlBWR12*, hw3740). Two sgRNAs were designed for each gene, and representative sequences of wild-type (WT) and corresponding mutant alleles (hw3710-CR1, hw3720-CR1, *SlBWR12*-CR1, *SlBWR12*-CR2, hw3740-CR1) are shown. sgRNA target sites are indicated in red, protospacer adjacent motif (PAM) sequences in blue, and deletions with dashed lines. **b**, Wilt symptoms of genome-edited (GE) tomato lines at 15 dpi. Scale bar, 10 cm. **c**, Disease severity index (DSI) over 20 days after soil drench inoculation with *R. pseudosolanacearum* (Ral) strain SL1944 (10^6 CFU g^{-1} soil). Repeated-measures ANOVA showed significant differences between *SlBWR12*-CR1 and the resistant control 'HW7996' (P = 0.0087), a significant effect of time (P = 0.0002), and a significant genotype × time interaction (P =

0.0018). **d**, Bacterial growth in the leaf at 0, 3, and 4 dpi following infiltration with Ral GMI1000 (gentamicin-resistant, 1×10^4 CFU mL^{-1}, 0.1 mL per leaf). Values, expressed as $\log_{10}$(CFU cm^{-2}), represent means ± standard deviation (s.d.) from three biological replicates, each quantified from four leaf discs. Gray, light blue, and blue bars indicate 0, 3, and 4 dpi, respectively. **e**, Wilt rate (%) of knockout lines inoculated with three Ral strains: SL882, SL1944, and GMI1000. **c,e**, Data show means ± standard error (s.e.) from three independent experiments, with 20–26 plants per replicate. Statistical significance was evaluated by Tukey's HSD test ($P < 0.05$).

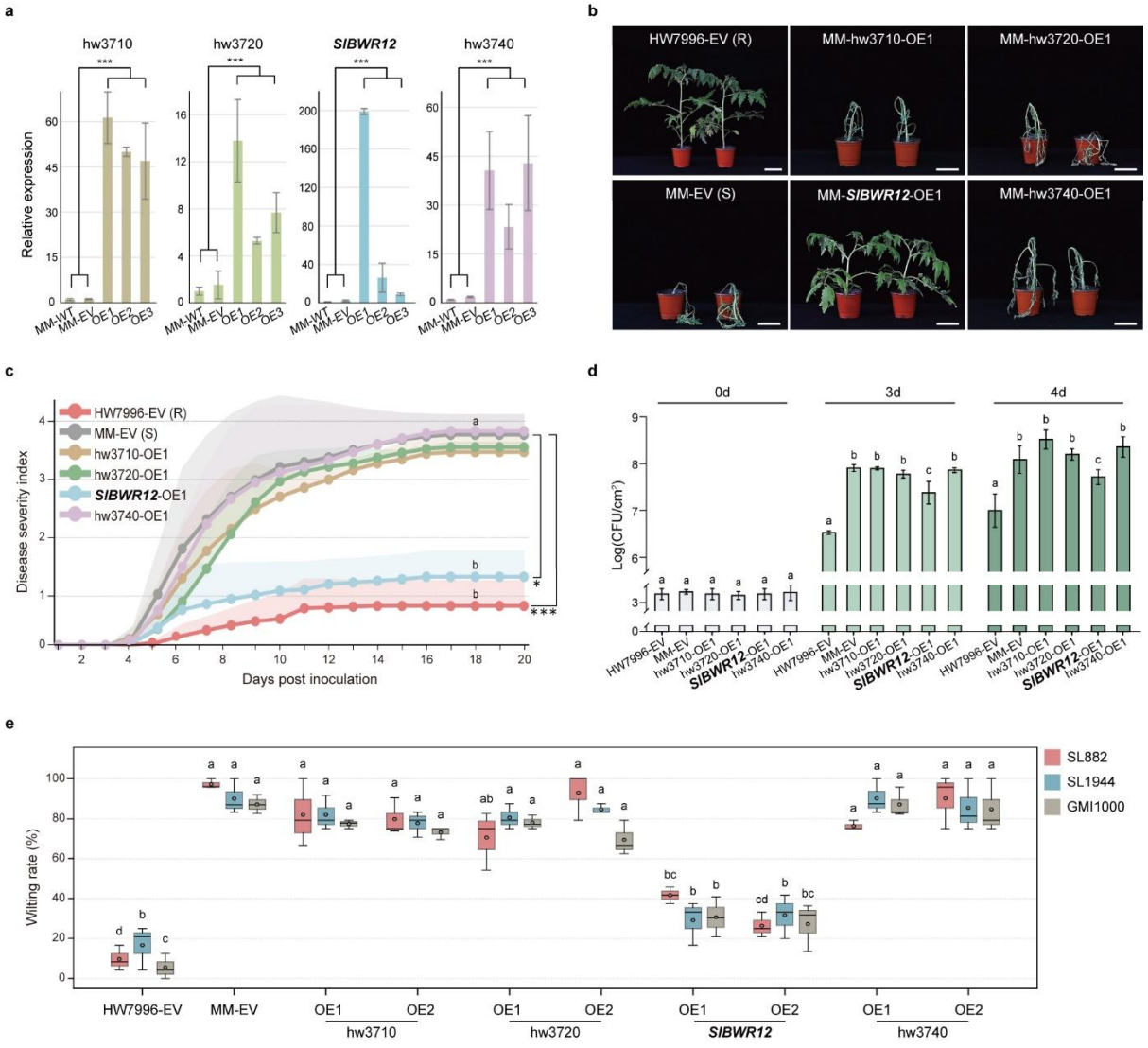
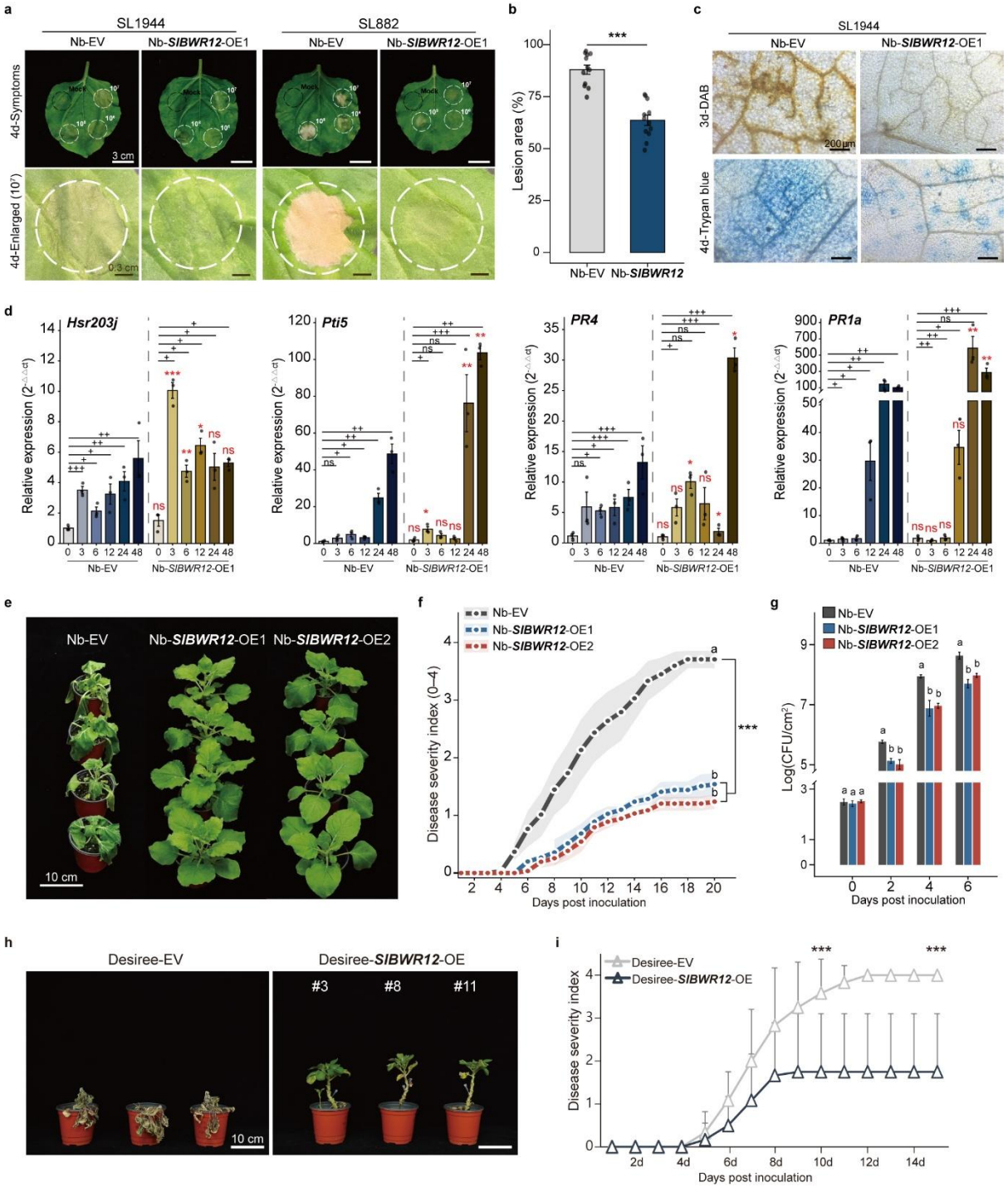


Figure 3. Identification of a bacterial wilt resistance gene among the four candidates by overexpression. a, Transcript levels of the four candidate RLP genes in overexpression (OE) lines. Three independent lines were analyzed per gene, and abundance was quantified from three plants per line. Data represent means ± s.d. (n = 3). Asterisks indicate significant differences compared with the susceptible control 'Moneymaker' ('MM') empty vector (MM-EV) (Student's t-test, ***, $P < 0.001$). **b**, Representative wilt symptoms of OE lines at 15 days post-inoculation (dpi). Scale bar, 10 cm. **c**, DSI over 20 days following soil drench inoculation with *R. pseudosolanacearum* (Ral) strain SL1944 (10^6 CFU g^{-1} soil). Repeated-measures ANOVA detected a significant difference between *SlBWR12*-OE1 and the susceptible control MM-EV ($P = 0.019$), a significant effect of time ($P = 4.0 \times 10^{-5}$), and a significant genotype × time interaction ($P = 5.9 \times 10^{-4}$). **d**, Bacterial populations in the leaf of OE and EV plants at 0, 3,

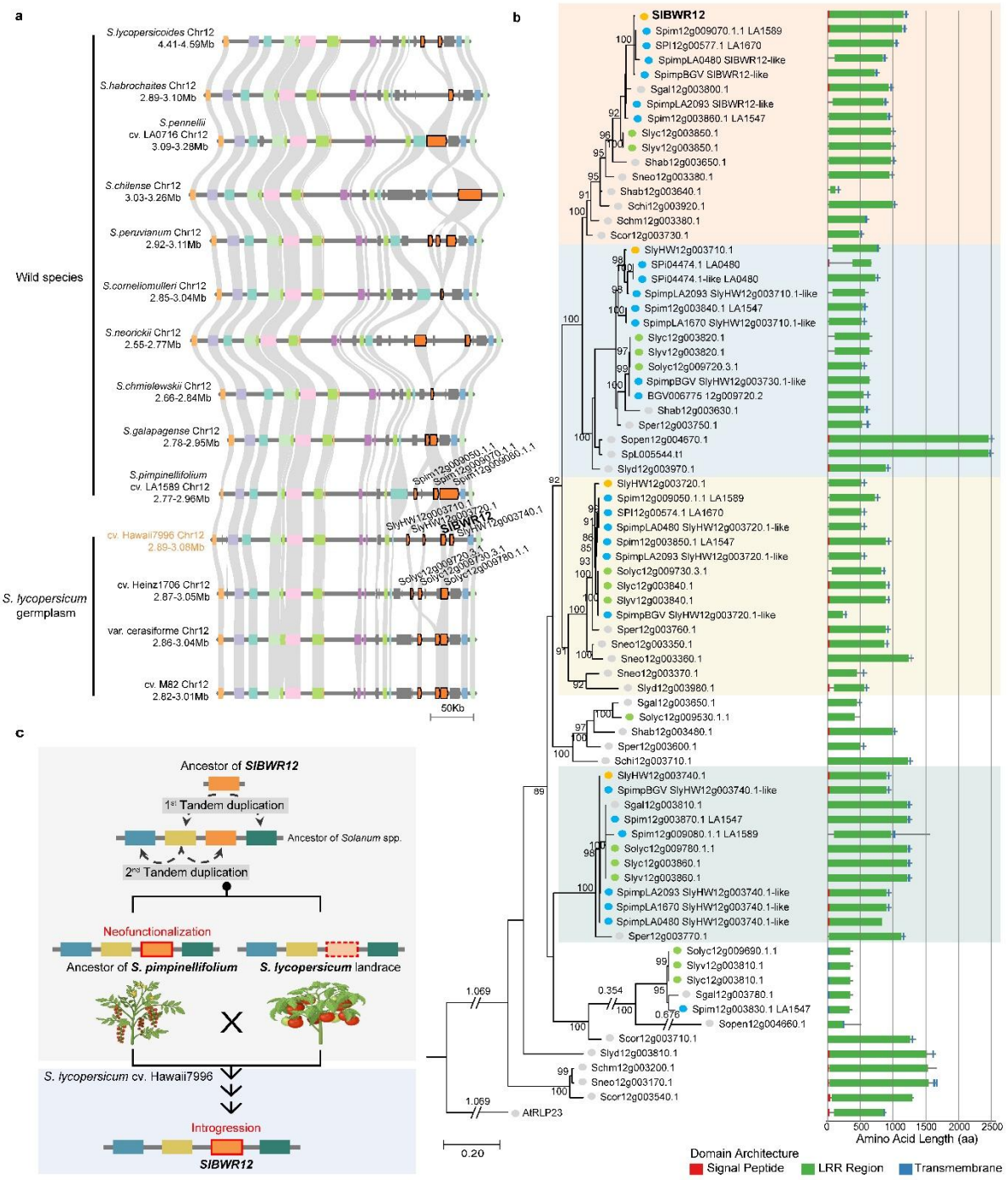
and 4 dpi following infiltration with Ral strain GMI1000 (gentamicin-resistant, 1×10^4 CFU mL^{-1}, 0.1 mL per leaf). Values are expressed as $\log_{10}$(CFU cm^{-2}) and represent means ± s.d. from three biological replicates, each averaged from four leaf discs. Gray, light green, and green bars correspond to 0, 3, and 4 dpi, respectively. **e**, Wilt rate (%) of OE lines inoculated with three Ral strains: SL882, SL1944, and GMI1000. **c–e**, HW7996-EV and MM-EV served as resistant and susceptible controls, respectively. Data represent means ± s.e. from three independent experiments, each using 20–26 plants per replicate. Statistical significance was assessed using Tukey's HSD test ($P < 0.05$).



1015

1016 **Figure 4. Functional characterization of *SlBWR12*-mediated bacterial wilt resistance in**
1017 ***Nicotiana benthamiana* and potato. a,** Representative leaves of empty vector (EV) and
1018 *SlBWR12*-overexpressing T_2 lines (OE-1) following leaf infiltration with *R.*
1019 *pseudosolanacearum* strains SL1944 and SL882 at 10^8, 10^7, and 10^6 CFU mL^{-1}. Scale bar, 3
1020 cm. Enlarged images show representative responses following infiltration at 10^7 CFU mL^{-1}.

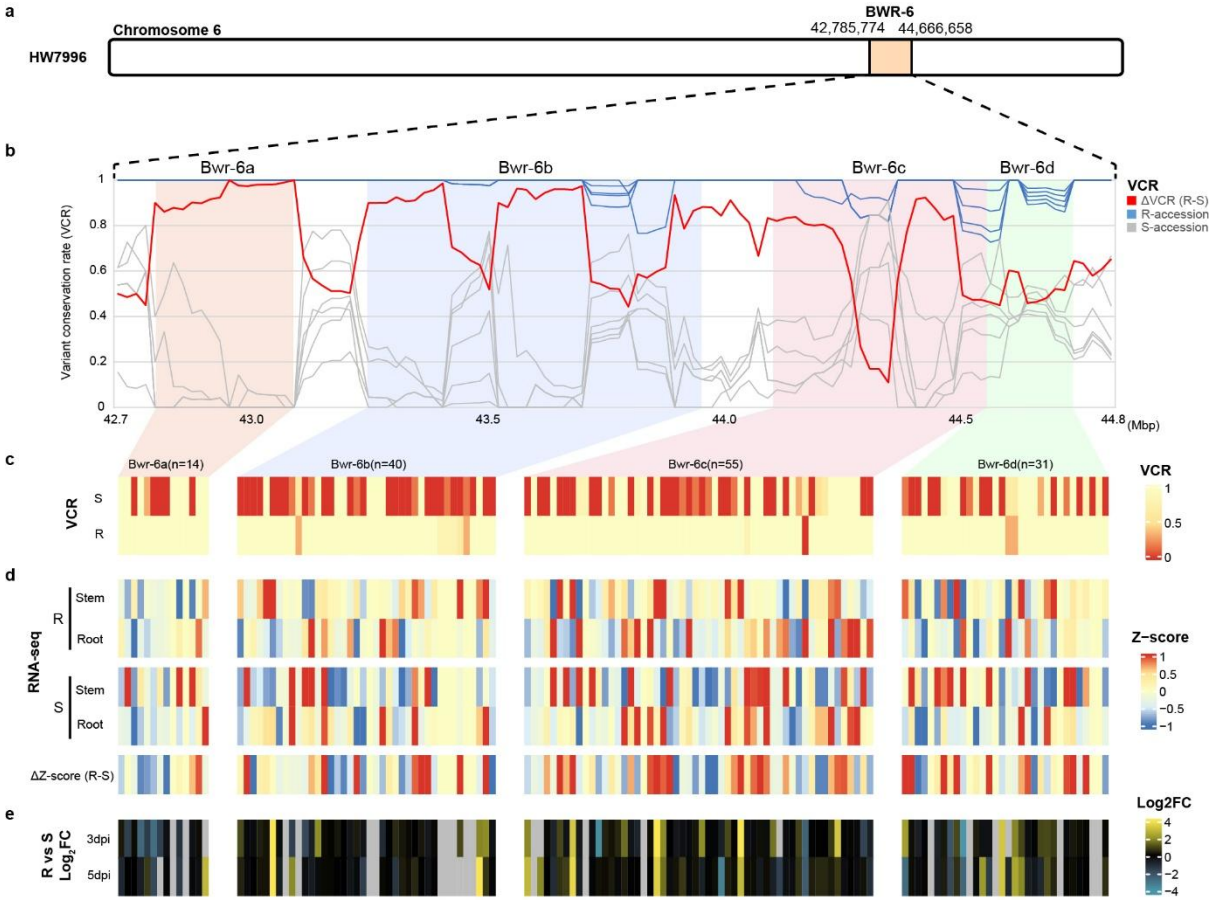
Scale bar, 0.3 cm. **b,** Quantification of lesion area in EV and OE-1 leaves following SL1944 infiltration. Data are presented as means ± s.d. Statistical significance was assessed using Student's t-test (***, $P < 0.001$). **c,** Representative DAB staining at 3 dpi and trypan blue staining at 4 dpi following SL1944 infiltration, showing ROS accumulation and cell death, respectively. **d,** Relative expression of the defense-related genes *Hsr203j*, *Pti5*, *PR4*, and *PR1a* in EV and OE-1 plants following SL1944 inoculation. Transcript levels were determined by RT–qPCR and calculated using the $2^{-\Delta\Delta Ct}$ method. Data are presented as means ± s.d. from three biological replicates. Statistical significance was assessed by two-way ANOVA. **e,** Representative disease phenotypes of EV, OE-1, and OE-2 plants following soil-drench inoculation with SL1944 at 2×10^6 CFU g^{-1} soil. **f,** Disease severity index (DSI) of EV, OE-1, and OE-2 plants following SL1944 soil-drench inoculation. Data are presented as means ± s.e. Statistical significance was assessed by two-way ANOVA followed by Tukey's HSD multiple-comparison test. **g,** Bacterial populations in the leaves of EV and *SlBWR12*-overexpressing T_2 plants following inoculation with SL1944. Values are expressed as log10(CFU cm^{-2}) and represent means ± s.e. Statistical significance was assessed by one-way ANOVA followed by Tukey's HSD multiple-comparison test. Different letters indicate significant differences among groups ($P < 0.05$). **h,** Bacterial wilt resistance conferred by *SlBWR12* in independent T_0 transgenic potato plants. Transgenic *Solanum tuberosum* cv. 'Desiree' plants overexpressing *SlBWR12* and empty vector (EV) controls were subjected to stem inoculation with *R. syzygii* SL2064 (phylotype IV). Each plant was inoculated with 5 µl of bacterial suspension (1×10^8 CFU ml^{-1}; 5×10^5 CFU per plant). Representative wilt symptoms were photographed at 10 dpi. Scale bar, 10 cm. **i,** Disease progression analysis in *SlBWR12*-overexpression potato lines. Disease severity index (DSI) of *SlBWR12*-overexpressing and EV control 'Desiree' plants monitored over 15 dpi. Data represent mean ± s.d. (n = 12 plants per genotype). Statistical analysis was performed using a linear mixed-effects model (LMM) ANOVA, with genotype and time as fixed effects and individual plants as random effects. All asterisks indicate significant differences where applicable (*$P < 0.05$; **$P < 0.01$; ***$P < 0.001$).



1048

1049 **Figure 5. Evolutionary analysis of the *SlBWR12* gene and its syntenic homologs. a**,
1050 Micro-synteny analysis of the chromosome 12 QTL region across 13 *Solanum* accessions,
1051 including 10 wild species and three landraces. Receptor-like protein (RLP) genes are
1052 highlighted in orange. Syntenic RLPs from *S. lycopersicum* 'Heinz1706' and *S. pimpinellifolium*
1053 'LA1589' are labeled accordingly. The synteny window spans a 50-kb genomic region. **b**,

Phylogenetic relationships and domain architecture of syntenic RLPs in the chromosome 12 region. Maximum-likelihood phylogeny of RLP genes within the syntenic interval is shown, including re-annotated genes from additional *S. pimpinellifolium* accessions. Genes from 'HW7996' are shown in orange, *S. pimpinellifolium* in blue, and *S. lycopersicum* in green. The shaded background denotes the 'HW7996' RLP gene cluster. Red, blue, yellow, and green indicate *SlBWR12*, *SlyHW12g003710.1*, *SlyHW12g003720.1*, and *SlyHW12g003740.1*, respectively. Corresponding domain architectures are illustrated alongside the phylogeny, with protein lengths indicated in amino acids (aa); red, green, and blue boxes represent the signal. peptide, leucine-rich repeat (LRR) region, and transmembrane (TM) domain, respectively. Scale bar represents 0.2 amino acid substitutions per site. **c**, Proposed evolutionary history of *SlBWR12* in 'HW7996'. A schematic model illustrating the inferred evolutionary trajectory of *SlBWR12* based on synteny, phylogenetic relationships, and copy-number variation across *Solanum* species.



Extended Data Fig. 1: Dissection of the chromosome 6 QTL region and identification of four candidate subregions associated with bacterial wilt resistance in tomato. a, The *Bwr-6* QTL interval mapped on chromosome 6 of 'HW7996'. **b**, Variant conservation density across the QTL region based on whole-genome resequencing. Variant frequencies were calculated using a 100-kb sliding window with a 10-kb step. Gray and blue lines represent susceptible and resistant accessions, respectively; the red line indicates the relative increase in variant frequency in resistant accessions vs. susceptible ones. The heatmap below shows the corresponding variant intensity. **c**, Heatmap of gene-level variation within the sub-region showing the highest accumulation of polymorphisms in **b**. Markers above the heatmap indicate marker names associated with each gene, with the number of genes per marker shown in parentheses. **d**, Expression profiles of the genes in **c**, represented as z-scores. **e**, Log_2 fold-change (log_2FC) values for the same gene set, showing differential expression between resistant and susceptible interactions.

Supplementary Files

This is a list of supplementary files associated with this preprint. Click to download.

- 261115SuppleFigure2.pdf
- 4.AppealNatcomSupplementaryTablev2.xlsx
- 261115SuppleFigure6.pdf
- 261115SuppleFigure13.pdf
- 261115SuppleFigure9.pdf
- 261115SuppleFigure3.pdf
- 261115SuppleFigure14.pdf
- 261115SuppleFigure10.pdf
- 261115SuppleFigure8.pdf
- 5.261113AppealNatcomSourcedata.zip
- 261115SuppleFigure7.pdf
- 261115SuppleFigure1.pdf
- 261115SuppleFigure12.pdf
- 261115SuppleFigure5.pdf
- 261115SuppleFigure4.pdf
- 261115SuppleFigure11.pdf
- 261115ExtendeddataFigure1.pdf